The protein kinase Akt acts as a coat adaptor in endocytic recycling

Jia-Wei Hsu[1,4], **Ming Bai**[1,4], **Kunhua Li**[2], **Jia-Shu Yang**[1], **Nam Chu**[3], **Philip A. Cole**[3], **Michael J. Eck**[2], **Jian Li**[1,5], **Victor W. Hsu**[1,5]

[1]Division of Rheumatology, Inflammation and Immunity, Brigham and Women's Hospital, and Department of Medicine, Harvard Medical School, Boston, MA 02115 USA

[2]Department of Cancer Biology, Dana-Farber Cancer Institute, and Department of Biological Chemistry and Molecular Pharmacology, Harvard Medical School, Boston, MA 02115 USA

[3]Division of Genetics, Brigham and Women's Hospital, and Departments of Medicine and Biological Chemistry and Molecular Pharmacology, Harvard Medical School, Boston, MA 02115 USA

[4]Equal contribution

Abstract

Coat proteins play a central role in vesicular transport by binding to cargoes for their sorting into intracellular pathways. Cargo recognition is mediated by components of the coat complex known as adaptor proteins[1–3]. We previously showed that ACAP1 (ArfGAP with Coil-coil Ankyrin repeat Protein 1) functions as an adaptor for a clathrin coat complex acting in endocytic recycling[4–6]. Here, we find that the protein kinase Akt acts as a co-adaptor in this complex, needed in conjunction with ACAP1 to bind cargo proteins for their recycling. Besides advancing the understanding of endocytic recycling, our findings uncover a fundamentally different way that a kinase acts, being an effector rather than a regulator in a cellular event.

Endocytic recycling is needed for a variety of cellular events, including cell motility and polarity, nutrient uptake, and signal transduction[7–12]. Recycling can occur either constitutively, for which the transferrin receptor (TfR) has been a model cargo[4], or in a stimulation-dependent fashion, for which integrin has been a model cargo[5]. We had previously found that ACAP1 acts as a coat adaptor for both types of recycling, transporting cargoes from the recycling endosome to the plasma membrane[4, 5]. For integrin recycling, we

further elucidated that ACAP1 binds to the β subunit of the α5β1 integrin heterodimer[13]. In considering whether another adaptor binds to the α5 subunit, we noted that the stimulation-dependent recycling of integrin requires serine at position 554 (S554) in ACAP1 to be phosphorylated by Akt[5]. However, whereas phosphorylation typically involves kinases associating transiently with their substrates, Akt associates more stably with ACAP1 for integrin recycling[5]. Thus, we explore the possibility that Akt could have a coat function.

We initially performed pulldown studies followed by immunoblotting, which revealed that ACAP1 does not bind directly to the cytoplasmic tail of multiple integrin α subunits that heterodimerize with β1 (Fig 1a and Extended Data Fig 1a). In contrast, direct binding is observed for Akt (Fig 1b and Extended Data Fig 1b). Moreover, the presence of Akt allows ACAP1 to associate with α tails (Fig 1c and Extended Data Fig 1c). We then assessed interactions through Coomassie staining, which revealed that Akt, either alone (Extended Data Fig 1d) or together with ACAP1 (Extended Data Fig 1e), binds efficiently to the α5 tail. The three components can also assemble efficiently into a complex in solution (Extended Data Fig 1f).

Akt has two major domains, a pleckstrin homology (PH) and a kinase domain. We found that only the kinase domain binds the α5 tail (Fig 1d and Extended Data Fig 1g) and ACAP1 (Fig 1e and Extended Data Fig 1h). For the latter interaction, Akt binds to the carboxyl portion of ACAP1, which contains the GTPase-activating protein (GAP) and ankyrin-repeat (ANK) domains of ACAP1 (Fig 1f and Extended Data Fig 1i). We also quantified the binding of the Akt kinase domain to the α5 tail (Fig 1g and Extended Data Fig 1j), and to ACAP1 (Fig 1h and Extended Data Fig 1k). Thus, the collective results suggested a model for how Akt could act as a co-adaptor with ACAP1 in cargo binding (Extended Data Fig 1l).

We next examined integrin recycling in cells. We had previously shown that mutating the S554 residue in ACAP1 to aspartate (S554D), which mimics its constitutive phosphorylation by Akt, results in integrin recycling becoming a constitutive process[5]. Thus, because the Akt kinase activity is no longer needed for integrin recycling in this situation[5], we revisited the S554D-expressing cells to examine whether Akt has a non-kinase role in integrin recycling. Upon siRNA against Akt (Extended Data Fig 2a), we found that integrin recycling in these cells is inhibited (Fig 1i and Extended Data Fig 2b). Moreover, this inhibition is rescued by not only the wild-type, but also the kinase-dead, form of Akt (Fig 1i and Extended Data Fig 2b). As integrin recycling mediates cell migration[7], we also found that siRNA against Akt inhibits cell motility, and this inhibition is also rescued by both wild-type and kinase-dead Akt (Extended Data Fig 3a). Furthermore, treatment with an Akt kinase inhibitor, GDC0068, does not inhibit integrin recycling in these cells (Extended Data Fig 3b). In contrast, integrin recycling in control cells is inhibited (Extended Data Fig 3c). We also detected an interaction between Akt and ACAP1 in cells (Fig 1j). Moreover, siRNA against Akt prevents endosomal integrin β1 from interacting with Akt and ACAP1 in the S554D-expressing cells, and this disruption is also rescued by both wild-type and kinase-dead Akt (Fig 1k). Thus, besides the previously elucidated kinase role[5], Akt also has a non-kinase role in integrin recycling.

Coat adaptors recognize specific sequences in cargoes, known as sorting signals, and mutating them inhibits cargo transport in the pathway governed by the coat complex[14]. As such, we next performed truncations followed by point mutagenesis to identify key residues in the α5 tail needed for its direct interaction with Akt (Fig 2a and 2b). We then mutated these residues (summarized in Fig 2c) in the full-length α5, and replaced endogenous α5 with the mutant α5 in cells. Examining integrin recycling (Fig 2d and Extended Data Fig 4a) and cell migration (Extended Data Fig 4b), we found that both are inhibited. Consistent with these findings, ACAP1 does not associate with the β1 integrin in cells that express the mutant, rather than the wild-type, α5 (Fig 2e). We also confirmed that the mutant α5 heterodimerizes with the wild-type β1 in cells (Fig 2f). Moreover, the resulting mutant integrin localizes to the recycling endosome in unstimulated cells (Fig 2g and Extended Data Fig 4c). Thus, the collective results revealed the importance of Akt interacting with the α5 tail for the recycling of the α5β1 integrin.

To test the broader relevance of our above results, we next examined TfR recycling, as it has been a general model for studies on endocytic recycling[8, 9, 12]. Upon siRNA against Akt in HeLa cells, we found that TfR recycling is also inhibited, which is again rescued by both wild-type and catalytic-dead Akt (Fig 3a and Extended Data Fig 5a). Similar results were also seen for TfR recycling in the human embryonic kidney (HEK) 293 cells (Extended Data Fig 5b). We also found that the siRNA treatment does not affect the internalization of surface TfR to the early endosome (Extended Data Fig 6a). Thus, the inhibition in TfR recycling cannot be attributed to an indirect effect of having affected TfR internalization.

The Akt kinase activity is stimulated by phosphorylation at two sites, threonine at position 308 (T308) and serine at position 473 (S473)[15]. Phosphorylation mutants have been generated that mimic the constitutive phosphorylation (T308D/S473D) and dephosphorylation (T308A/S473A) at these sites[16]. We found that the inhibition of TfR recycling induced by siRNA against Akt is rescued similarly by either Akt phosphorylation mutant (Extended Data Fig 6b). Treatment with the Akt kinase inhibitor, GDC0068, also does not affect TfR recycling (Extended Data Fig 7a). Thus, these results further supported a non-kinase role for Akt in TfR recycling. As we had thus far been using an siRNA oligonucleotide that targets a common sequence in Akt1 and Akt2, we also assessed the relative contribution of the two Akt isoforms in TfR recycling. Treating cells with siRNA that targets either Akt1 or Akt2, we found that either treatment reduced the total Akt level partially (Extended Data Fig 7b), and this correlates with partial inhibition of TfR recycling (Extended Data Fig 7c and Extended Data Fig 7d), suggesting that both Akt isoforms participate in TfR recycling.

We next found that Akt also binds directly to the cytoplasmic domain of TfR (Fig 3b). Moreover, an α5 cargo peptide competes with this binding (Fig 3c), suggesting that Akt has a common binding site for both TfR and α5. To further test whether Akt acts in the cargo sorting of TfR for its recycling, we next determined whether the sequence in TfR recognized by Akt functions as a recycling sorting signal. We had previously found that ACAP1 binds to two sites in the TfR cytoplasmic domain, with one site residing within the amino portion (containing the first 19 residues, N19) and the other site residing in the remaining portion (N 19)[4] (summarized in Extended Data Fig 8a). We found that Akt binds to both constructs

(Fig 3d). We then performed alanine-scanning mutagenesis to identify critical residues in either construct needed for Akt binding (Fig 3e and 3f). Notably, the identified residues are the same ones that we had previously elucidated to be required for TfR recycling[4]. Thus, the collective observations suggested that Akt binds to recycling sorting signals in TfR.

However, we had also found previously that ACAP1 binds to the identical two sites in TfR[4], which suggested seemingly that ACAP1 and Akt would compete against each other for binding to TfR. Pursuing a reconciling explanation, we next titrated increasing level of ACAP1 for incubation with either the N19 construct or the N 19 TfR construct in pulldown studies, and found that Akt binds preferentially to the N19 construct (Fig 3g), while ACAP1 binds preferentially to the N 19 construct (Fig 3h). We next generated fusion proteins that contain the cargo-binding portions of ACAP1 (GAP-ANK domains) or Akt (kinase domain), having homodimers of either the ACAP1 or Akt domains, or a heterodimer containing both Akt and ACAP1 domains. Performing pulldown studies, we fund that the heterodimer exhibits greater affinity to the TfR cytoplasmic domain than that of either homodimer (Extended Data Fig 8b). We also found that siRNA against Akt disrupts the association of ACAP1 with endosomal TfR in cells (Extended Data Fig 8c). Similarly, siRNA against ACAP1 disrupts the association of Akt with endosomal TfR in cells (Extended Data Fig 8d). Thus, the collective results confirmed that ACAP1 and Akt act cooperatively in binding to TfR.

Besides binding to cargoes, coat adaptors also link clathrin to cargoes in coat complexes[1]. Thus, to examine whether Akt also acts in this capacity, we initially elucidated that the kinase, but not the PH, domain of Akt binds directly to clathrin (Fig 4a). We then found that, whereas neither the α5 nor the TfR cytoplasmic domain can bind directly clathrin, the addition of the Akt kinase domain allows clathrin to form complexes with either cargo (Fig 4b). We also found that the additional presence of ACAP1 enables clathrin to associate with the TfR cytoplasmic domain more efficiently (Fig 4c). Moreover, co-precipitation studies revealed that siRNA against Akt disrupts the association of ACAP1 with clathrin in cells (Fig 4d), while siRNA against ACAP1 disrupts the association of Akt with clathrin (Fig 4e). Thus, Akt also behaves as a co-adaptor with ACAP1 in linking clathrin to cargoes.

We had previously found that the small GTPase ADP-Ribosylation Factor 6 (ARF6) regulates the recruitment ACAP1 to the recycling endosome[6]. Thus, to determine whether ARF6 regulates the recruitment of Akt similarly, we isolated a membrane fraction enriched for the recycling endosome (Extended Data Fig 9a). Initially, we found that Akt alone cannot be recruited to this membrane (Extended Data Fig 9b). However, ARF6 in its activated form can be recruited to this membrane (Extended Data Fig 9c). We then found that activated ARF6 is needed to recruit Akt (Fig 4f) and ACAP1 (Fig 4g) to this membrane. Moreover, activated ARF6 alone cannot recruit clathrin to this membrane (Fig 4h), but requires the presence of Akt and ACAP1 (Fig 4h and Extended Data Fig 9d). Thus, Akt and ACAP1 also act as co-adaptors in recruiting clathrin to endosomal membrane. The recruitment of all coat components onto membrane can also be reconstituted using liposomes, which revealed that they assemble on membrane at nearly stoichiometric levels (Extended Data Fig 9e).

We next pursued cell-based studies. Initially, we found that endogenous Akt exhibits a diffuse distribution, having only a minimally detectable pool at the recycling endosome (Fig 5a). This finding was confirmed by staining using another antibody against Akt (Extended Data Fig 10a). As one explanation, we found by cell fraction that Akt exists mostly in the cytosol (Fig 5b). We then elucidated a complementary explanation. Pursuing a more denaturing condition of cell fixation, we found that Akt at the recycling endosome can be detected more efficiently (Fig 5c). Moreover, as the harsher fixation protocol did not affect the detection of clathrin at the recycling endosome (Extended Data Fig 10b), the collective observations suggested that Akt at the recycling endosome is mostly assembled into complexes that hinder its detection by antibody.

To further support this conclusion, we revisited the ARF6-dependent recruitment of Akt, ACAP1, and clathrin onto endosomal membrane. This time, we added an Akt antibody after the recruitment in two ways, either before or after membrane solubilization with detergent. Upon isolating the Akt antibody, we found that more Akt is detected in the latter condition (Fig 5d). As comparison, when only Akt is recruited to endosomal membrane by ARF6, we found that the Akt antibody detects similar levels of membrane-bound Akt, regardless of whether the antibody is added before or after membrane solubilization with detergent (Fig 5e). Thus, these results further supported that Akt at the recycling endosome exists mostly in assembled complexes that impair Akt detection by its antibody.

We then noted that ARNO (ARF nucleotide binding site opener) has been shown to act as an ARF6 GEF (guanine nucleotide exchange factor) in endocytic recycling[17]. Upon ARNO overexpression, we observed enhanced recruitment of Akt to the recycling endosome, as reflected by its enhanced detection through antibody staining (Fig 5f). The catalytic activity of ARNO is needed for this enhanced recruitment (Fig 5f). We also found that Akt staining is reduced by the overexpression of the mutant ARNO (Fig 5f), which is explained by the mutant ARNO be able to localize similarly to the recycling endosome as the wild-type form (Extended Data Fig 10c), resulting in a dominant negative effect on Akt recruitment to the recycling endosome. We further discovered that cell stimulation does not have an appreciable effect on the pool of Akt at the recycling endosome (Extended Data Fig 10d). Thus, in contrast to Akt recruitment to the plasma membrane, which is regulated by growth factors[15], and has been shown to induce Akt into clathrin complexes at the cell surface that act in endocytosis[18], Akt recruitment to the recycling endosome is regulated differently, modulated instead by ARF6 and its GEF, which results in Akt assembled into clathrin complexes on endosomal membrane that act in recycling.

In summary, we have uncovered a non-kinase role of Akt, acting as a coat adaptor in endocytic recycling. An intriguing implication also arises from this discovery. Many kinases have now been identified to act in different intracellular transport pathways. Currently, these kinases are only known to act as regulators, which involves their kinase activity that phosphorylates downstream targets to modulate function[19–26]. Our finding that Akt acts as a coat adaptor in endocytic recycling raises the prospect that this fundamentally different role, acting as an effector rather than as a regulator, may be more widespread across the intracellular pathways than currently appreciated.

METHODS

Chemicals and proteins.

GDP and GTPγS were obtained from Sigma. Protein A/G agarose beads were obtained from Pierce. The Akt kinase inhibitor GDC0068 was obtained from BioVision. Integrin α5 peptides (wild-type: KLGFFKRSLPYG, mutant: KLGAAAASLPYG) were synthesized by GenScript. Alexa 546-conjugated transferrin was obtained from Invitrogen. GST fusion proteins expressed through bacterial expression were purified as described previously[4]. The generation of recombinant ARF6 and ACAP1 have also been described[4, 6]. Purified clathrin was a kind gift from T. Kirchhausen (Harvard Medical School, USA). For all studies using Akt as a recombinant protein, Akt1 was used. Recombinant Akt1 forms were generated using the Bac-to-Bac Baculovirus Expression System (Invitrogen). Briefly, infected Sf9 cells were resuspended in hypotonic buffer (20 mM Tris pH 8.0, 100 mM NaCl, 1mM EDTA and protease inhibitor) followed by lysis using sonication. For 6xHis-tagged Akt1 forms, after binding with Ni-NTA resin, proteins were eluted with buffer containing 500 mM imidazole and then dialyzed using storage buffer (25 mM Tris pH7.5, 100 mM NaCl). For GST-tagged Akt1 forms, after binding with glutathione agarose resin, proteins were eluted with buffer containing 10mM glutathione, 50mM Tris pH8.0, and 200mM NaCl and then dialyzed using storage buffer (25mM Tris pH7.5, 100mM NaCl).

Cells and transfections.

HeLa and HEK293 cells were obtained from the American Type Culture Collection (ATCC) and maintained in Dulbecco's Modified Eagle Medium (DMEM) with 10% fetal bovine serum (FBS) and supplemented with glutamine and penicillin/streptomycin. DNA plasmids were transfected using FuGene6 (Roche). Oligonucleotides for siRNA experiments were transfected using PepMute (SignaGen).

Antibodies.

The following antibodies were generated by us[4–6] : rabbit antisera against ACAP1 (WB 1:500), ARF6 (WB 1:500), and cellubrevin (IF/WB 1:500). The following antibodies were obtained from other investigators: mouse TS2/16 against integrin beta1 (L. Klickstein, Brigham and Women's Hospital, USA; IF/IP/WB 1:5) and mouse 9E10 against the Myc epitope (R. Klausner, National Institutes of Health, USA; IP/WB 1:500). The following antibodies were obtained from commercial sources: GST (Santa Cruz; sc-138, 1:200), 6xHis (Santa Cruz; sc-803, WB 1:200), Akt (Cell Signaling; 9272, IF/WB 1:1000; 2920, IF 1:1000), β-actin (Ambion; AM4302, WB 1:1000), Rab11 (BD Biosciences; 610656, IF 1:100), and mouse TD.1 (American Type Culture Collection; WB 1:5) and X22 (American Type Culture Collection; IF 1:5) against clathrin. Conjugated secondary antibodies were obtained from Jackson ImmunoResearch: horseradish peroxidase-conjugated donkey antibodies against mouse IgG (715-035-150, WB 1:10,000) and against rabbit IgG (711-035-152, WB 1:10,000), Cy2 donkey antibodies against mouse IgG (715-225-151, IF 1:200) and against rabbit IgG (711-225-152, IF 1:200), Cy3 goat antibody against mouse IgG (115-165-062, IF 1:200), and Cy3 donkey antibodies against rabbit IgG (711-165-152, IF 1:200).

Plasmids.

Myc-tagged ACAP1 has been described previously[5]. Akt forms, wild-type, catalytic dead (K179M), and phosphorylation mutants (T308D/S473D and T308A/S473A) were gifts from Alex Toker (Beth Israel Deaconess Medical Center, Boston, MA). ARNO forms, wild-type and catalytic dead (E156K), in pcDNA3 were gifts from Lorraine Santy (Pennsylvania State University, University Park, PA). The following GST fusion constructs have been described previously: GST-α5 forms (full-length and truncations)[13], GST-TfR forms (full-length and truncations)[4], and GST-ACAP1 forms (BAR-PH and GAP-ANK)[13]. GST-Akt forms (full-length and truncations) were subcloned into the BamHI and XhoI sites of the pFastBac™HT plasmid (Invitrogen), followed by baculovirus expression as described above. 6xHis-tagged Akt kinase domain was subcloned into the BamHI sites of the pET15b vector for bacterial expression.

Sequences for siRNA.

Sequence for siRNA against ACAP1 is CACAAGCTGGACAGCCATG. Sequences for siRNA against Akt1 and Akt2 are CCAGGACCATGAGAAGCTT and CCAGGACCACGAGCGCCTC, respectively. Sequence for siRNA that target a common sequence in Akt1 and Akt2 is TGCCCTTCTACAACCAGGA. Sequence for shRNA against integrin α5 is CCACAGATAACTTCACCCGAA. Rescue plasmids were generated using QuikChange Site-Directed-Mutagenesis (Stratagene). Oligonucleotide sequences used to generate siRNA resistant Akt1/2 are:
ATGATGTGCGGTCGCCTCCCGTTTTATAATCAAGACCATGAGAAGCTTTTTGAG (forward) and
CTCAAAAAGCTTCTCATGGTCTTGATTATAAAACGGGAGGCGACCGCACATCAT (reverse). Oligonucleotide sequences used to generate shRNA resistant α5 integrin are:
GCTACCTCTCCACAGACAATTTTACCCGAATTCTGGAG (forward) and
CTCCAGAATTCGGGTAAAATTGTCTGTGGAGAGGTAGC (reverse).

Pulldown studies.

GST fusion proteins on glutathione beads were incubated with soluble proteins (100 nM) at 4°C for 1 hour in incubation buffer (PBS with 0.5% Triton X-100). Beads were then pelleted by centrifugation at 800x *g* for 2 minutes at 4°C, followed by two washes with incubation buffer. Samples were then analysis by SDS-PAGE followed by either Coomassie staining or western blotting.

To detect a complex that contains GST-α5, Akt, and ACAP1, all three components were incubated as soluble proteins at 200 nM, followed by isolation on glutathione beads. Beads were then analyzed by SDS/PAGE followed by Coomassie staining.

Biolayer interferometry.

Analysis was performed with ForteBio Octet RED384 instruments and ForteBio biosensors. Data analyses used ForteBio Data Analysis 11.1 HT. Kinetics assays were carried out in Kinetic Buffer (PBS+ 0.02% Tween20, 0.1% BSA, 0.05% sodium azide) at 30°C using settings of Standard Kinetics Acquisition rate (5.0 Hz, averaging by 20) at a sample plate shake speed of 1000 rpm. The Ni-NTA (Molecular Devices, 18–5101) sensors were loaded

with His-tagged Akt kinase domain (residue range 144–480, 25 μg/ml) and then dipped into wells containing GST-α5 or GST-ACAP1 domain (GAP-ANK) at various concentrations to monitor analyte association. The dissociation step was monitored by dipping sensors back into the wells contains blank Kinetic Buffer. Double reference subtracted binding curves were analyzed to obtain binding constant (Kd) values. All binding experiments were performed in duplicate.

Subcellular fractionation.

Cells were washed with PBS, resuspended in homogenization buffer (0.25 M sucrose, 1 mM EDTA, and 20 mM HEPES-KOH, pH 7.4 and protease inhibitor cocktail) and then incubated on ice for 15 minutes before passing through a 25-gauge needle to obtain cell homogenates. After centrifugation (800x g for 6 minutes) to pellet nuclei and unbroken cells, the post-nuclear supernatant was centrifuged at 100,000x g for 1 hour to obtain total membrane and cytosol. Equal fractional amounts were then analyzed by SDS/PAGE followed by western blotting.

Isolation of membrane enriched for the recycling endosome.

HeLa cells were collected and resuspended in homogenization buffer (320 mM sucrose and 25 mM Tris pH 7.4). Cells were homogenized using a ball-bearing homogenizer with 25 μm clearance, and then subjected to centrifugation at 2000x g for 10 minutes. The resulting supernatant was loaded onto the top of a sucrose step gradient that contains 29% sucrose (top) and 35% sucrose (bottom). Centrifugation was then preformed at 110,000x g for 2.5 hours. Endosome membrane fraction was collected at the 29% and 35% sucrose interface.

Nucleotide loading of ARF6.

Recombinant ARF6 was loaded with GTPγS or GDP in a nucleotide exchange buffer (50 mM HEPES-KOH pH7.5, 100 mM KCl, 1 mM DTT, 0.5 mM $MgCl_2$, 1 mM EDTA and 10 uM GTPγS or 100uM GDP) at 30° C for 30 minutes. Reaction was then terminated by increasing the $MgCl_2$ content (10 mM final concentration) to stabilize the nucleotide bound state.

Recruitment of coat components onto endosomal membrane.

Endosome-enriched membrane was pre-washed with 3M KCl buffer on ice for 10 minutes. The washed membrane (0.2 mg/ml) in 500 ul of traffic buffer (25 mM HEPES pH 7.2, 50 mM KCl, 2.5 mM Mg(OAc)$_2$, and 200 mM sucrose) was then incubated for 1 hour at room temperature with 100 nM of different coat components as specified in the figure legend. Samples were centrifuged for 10 minutes at 12,000x g to recover endosomal membrane in the pellet (P) fraction. The supernatant (S) fraction was concentrated by TCA precipitation. Equal fractional amounts were then analyzed by western blotting.

Recruitment of coat components onto liposomes.

Liposomes that mimic endosomal lipid composition (58% phosphatidylcholine, 4% phosphatidylserine, 20% phosphatidylethanolamine, 14% cholesterol, 4% sphingomyelin, 1% phosphatidylinositol 4,5-bisphosphate, and 1% phosphatidylinositol 3,4,5-trisphosphate)

and having 400 nm diameter were generated in traffic buffer (25 mM HEPES pH 7.2, 50mM KCl, 2.5 mM Mg(OAc)$_2$, 200 mM sucrose) and resuspended in this buffer without sucrose (25 mM HEPES pH 7.2, 50mM KCl, 2.5 mM Mg(OAc)$_2$) at 1 μg/μl. Liposomes (0.4 μg/μl) were then incubated with 300 nM of clathrin, ACAP1, Akt and GTPγS-loaded Arf6 in traffic buffer without sucrose at 37° C for 20 minutes, followed by centrifugation at 13,000 × g for 20 minutes at 4° C to pellet liposomes. Both the pellet and supernatant fractions were then assessed by Coomassie staining.

Co-precipitation studies.

Immunoprecipitation of endosomal β1 has been described previously[5]. Briefly, an anti-β1 antibody was incubated with serum-starved cells to bind the surface pool of integrin β1 at 4°C for 1 hour. After washing away unbound antibody, cells were incubated at 37°C for 2 hours to allow the antibody-bound surface pool of β1 to accumulate at the recycling endosome. Cells were subjected to lysis buffer (1% Triton X-100, 20 mM Tris pH 7.4, and 300 mM NaCl) and then incubated with protein A coated beads. Beads were then washed three times with lysis buffer, and then analyzed by SDS/PAGE followed by western blotting.

Immunoprecipitation of endosomal TfR has also been described previously[5]. Briefly, cells were incubated with biotin-conjugated Tf at 37°C for 2 hours to label TfR at the cell surface and in endosomal compartments. Cells were then washed with an acidic buffer (0.5M NaCl and 0.5% acetic acid) to release biotin-Tf bound to TfR at the cell surface. Cells were then lysed and then incubated with streptavidin agarose beads at 4°C for 2 hours. Beads were then washed three times with lysis buffer and then analyzed by SDS-PAGE followed by western blotting.

For immunoprecipitation of ACAP1-myc, HeLa cells were transfected with this construct, and then disrupted in lysis buffer (PBS with 0.5% TX-100 and protease inhibitors). Lysates were cleared by centrifugation at 16,000 × g for 15 minutes at 4°C, and then incubated with an anti-Myc antibody for 2 hours at 4°C followed by incubation with protein A beads. Beads were then washed three times with lysis buffer and then analyzed by western blotting.

Transport assays.

The TfR endocytosis and recycling assays have been described previously[27]. Briefly, for TfR endocytosis, cells were incubated with Alexa 546-conjugated Tf (5μg/ml in DMEM) for 1 hour at 4°C. Cells were then washed to clear unbound Tf, followed by shifting to 37°C for different time points. Cells were stained for EEA1, followed by confocal microscopy to assess the arrival of Tf to the early endosome.

For TfR recycling, cells were incubated with Alexa 546-conjugated Tf (5μg/ml in DMEM without serum) at 37°C for 2 hours to label TfR in endosomal compartments. Cells were then incubated with complete medium (which contains unlabeled Tf) at 37°C for different time points. After staining for a recycling endosome (RE) marker (Rab11 or cellubrevin), cells were analyzed by confocal microscopy to quantify the colocalization of labeled TfR with RE marker at different time points.

The integrin recycling assay to track the stimulation-dependent recycling of integrin β1 in HeLa cells has been described[5]. Briefly, serum-starved cells were incubated with an anti-β1 antibody at 4°C for 1 hour to bind the surface pool of integrin β1. After washing away unbound antibody, cells were incubated at 37°C for 2 hours to allow the antibody-bound pool of surface β1 to accumulate at the recycling endosome. Upon serum stimulation, cells were then analyzed by confocal microscopy to quantify the colocalization of endosomal integrin β1 with RE marker at different time points.

The integrin recycling assay to track the constitutive recycling of integrin β1 in cells that express the S554D mutant ACAP1 has also been described[5]. Briefly, cells were incubated with an anti-β1 antibody at 4°C for 1 hour to bind the surface pool of integrin β1. After washing away unbound antibody, cells were incubated at 37°C for 2 hours in the presence of primaquine to allow the antibody-bound pool of surface β1 to accumulate at the recycling endosome. Upon washout, cells were then analyzed by confocal microscopy to quantify the colocalization of endosomal integrin β1 with RE marker at different time points.

Note that integrin recycling exhibits a "V"-shaped curve in the quantitative assay, because stimulation induces endosomal integrin (which had been gathered at the RE in the serum-starved condition) to cycle between the RE and the plasma membrane. Thus, because the antibody remains bound to the integrin, the assay tracks the entire cycling itinerary of the endocytic integrin[28]. On the other hand, TfR recycling exhibits only a downward slope in the quantitative assay, because Tf becomes released from TfR when endosomal TfR reaches the plasma membrane, for which a more detailed explanation has been provided previously[9].

For both integrin and TfR recycling, GDC0068 was added at 200 nM for 1 hour to assess the role of the Akt kinase activity.

Confocal microscopy.

Colocalization studies were performed using a Zeiss system equipped with the Axio Observer Z1 Inverted Microscope, having a Plan-Apochromat 63x objective, coupled to the LSM 800 confocal system with Airyscan package, and the Zen 2.3 blue edition confocal acquisition software.

For quantification of colocalization, ten fields of cells were examined, with each field typically having 5 cells. Images were imported into the NIH Image J (version 1.50i) software with colocalization plugin (https://imagej.net/Coloc_2) for analysis. The threshold values were chosen automatically by the program based on the Costes method. Manders' coefficients were then calculated and expressed as the fraction of protein of interest (cargo protein or Akt) colocalized with a compartmental marker.

Cell migration assay.

Cell migration using a transwell chamber (Corning #3422) has been described previously[5]. Briefly, HeLa cells were plated onto the fibronectin-coated membrane in the transwell chamber, and then allowed to migrate for 4 hours at 37°C. To detect cells that have migrated across the membrane, cells were stained with DAPI (4',6-diamidino-2-phenylindole) and then quantified using fluorescence microscopy.

Statistics and Reproducibility.

Quantitative data are shown as mean with standard deviation. Statistical significance was determined using the paired two-tailed Student's t-test, through Prism (version v7.04) or Excel (version Office 2016) software. The sample number (n) indicates the number of independent biological experiments. For quantitative colocalization studies that involve n=3, the mean for each experiment was first determined by examining 10 cells per experiment. Subsequently, these values were used to determine the mean with standard deviation for the quantitative data shown in figures. The following figures have independent biological experiments with n=2: Figure 1a–h, 1j–k, 2a–b, 2e–f, 3b–h, 4a–h, Extended Data Figure 1a–k, 2a, 7b, 8b–d, 9a–e. All other figures, except for illustrations (Figure 2c, and Extended Data Figure 1l and 8a), have independent biological experiments with n=3.

Extended Data
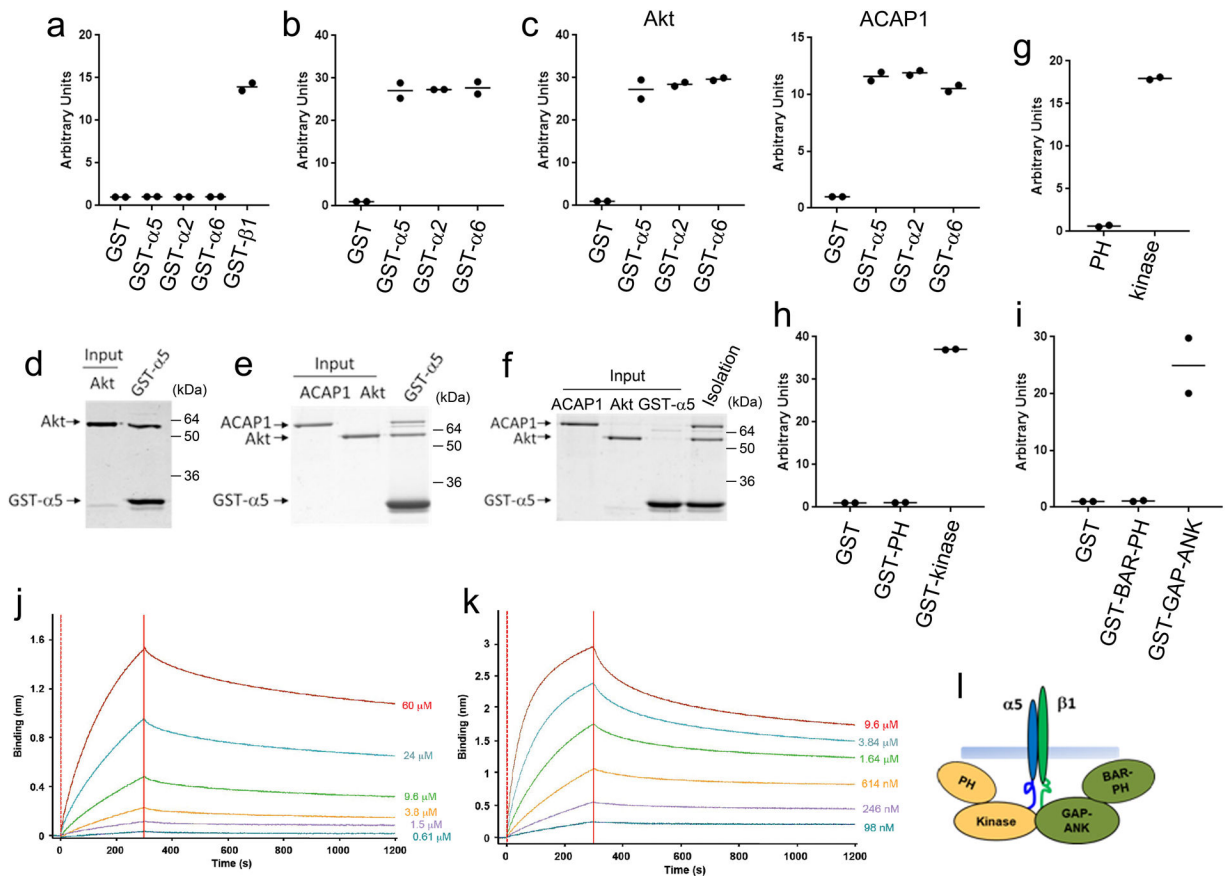
Extended Data Fig. 1. Further characterizing cargo binding interactions.
a, b, c, Pulldown interactions from 2 independent experiments are quantified for studies shown in Figure 1a (**a**), in Figure 1b (**b**), and in Figure 1c (**c**). Data available in Source Data Extended Data Fig 1a, 1b, 1c. **d, e,** Pulldown studies followed by Coomassie staining to detect soluble forms Akt bound to GST-α5 on beads (**d**) or soluble Akt and ACAP1 bound to GST-α5 on beads (**e**); n= 2 independent experiments. Input shows 10% of soluble components used in the incubation. Data available in Unprocessed Blots Extended Data Fig 1d, 1e. **f,** A soluble complex containing GST-α5, Akt, and ACAP1 is detected by incubating the three components in solution, followed by isolation using glutathione beads, and then Coomassie staining to assess complex formation; n= 2 independent experiments. Input shows 10% of soluble components used for the incubation. Data available in Unprocessed Blots Extended Data Fig 1f. **g, h, i,** Pulldown interactions from 2 independent experiments are quantified for studies shown in Figure 1d (**g**), in Figure 1e (**h**), and in Figure 1f (**i**). Data available in Source Data Extended Data Fig 1g, 1h, 1i. **j, k,** Primary data for biolayer interferometry measurements that quantify the interaction between GST-α5 and the Akt kinase domain shown in Figure 1g (**j**), and between the Akt kinase domain and the carboxyl portion of ACAP1 shown in Figure 1h (**k**); n= 2 independent experiments. **l,** A model for how Akt and ACAP1 act as co-adaptors in binding to the α5β1 integrin heterodimer.
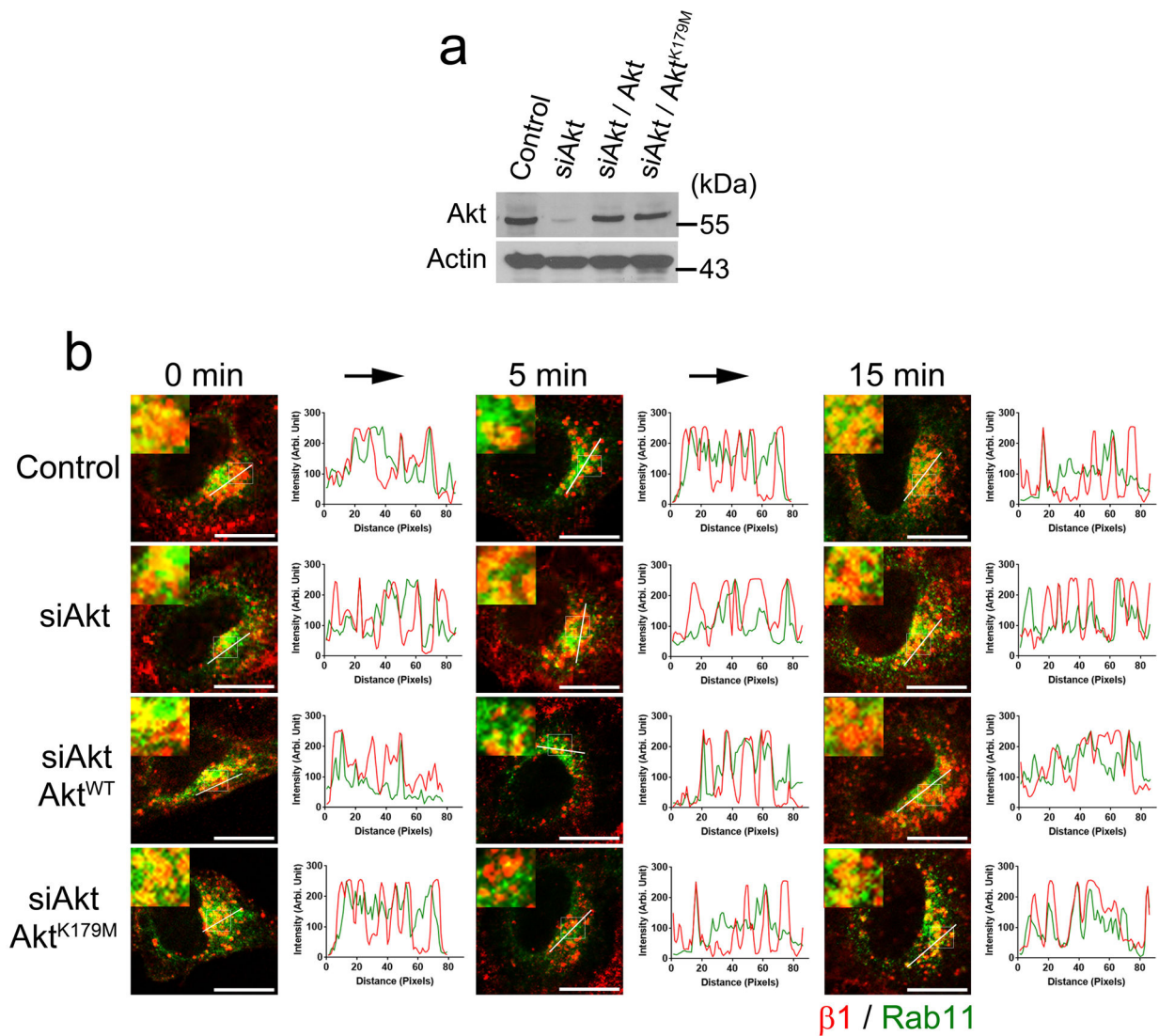
Extended Data Fig. 2. Akt having a non-kinase role in integrin recycling.
a, Efficiency of siRNA against Akt and its rescues in HeLa cells that express the ACAP1 mutant (S554D), as detected by immunoblotting of whole cell lysates; n= 2 independent experiments. Data available in Unprocessed Blots Extended Data Fig 2a. **b,** Representative primary images from the integrin recycling assay shown in Figure 1i; n= 3 independent experiments. The colocalization of endosomal β1 with Rab11, a marker of the recycling endosome, is assessed; β1 (red), Rab11 (green), bar = 10 um.
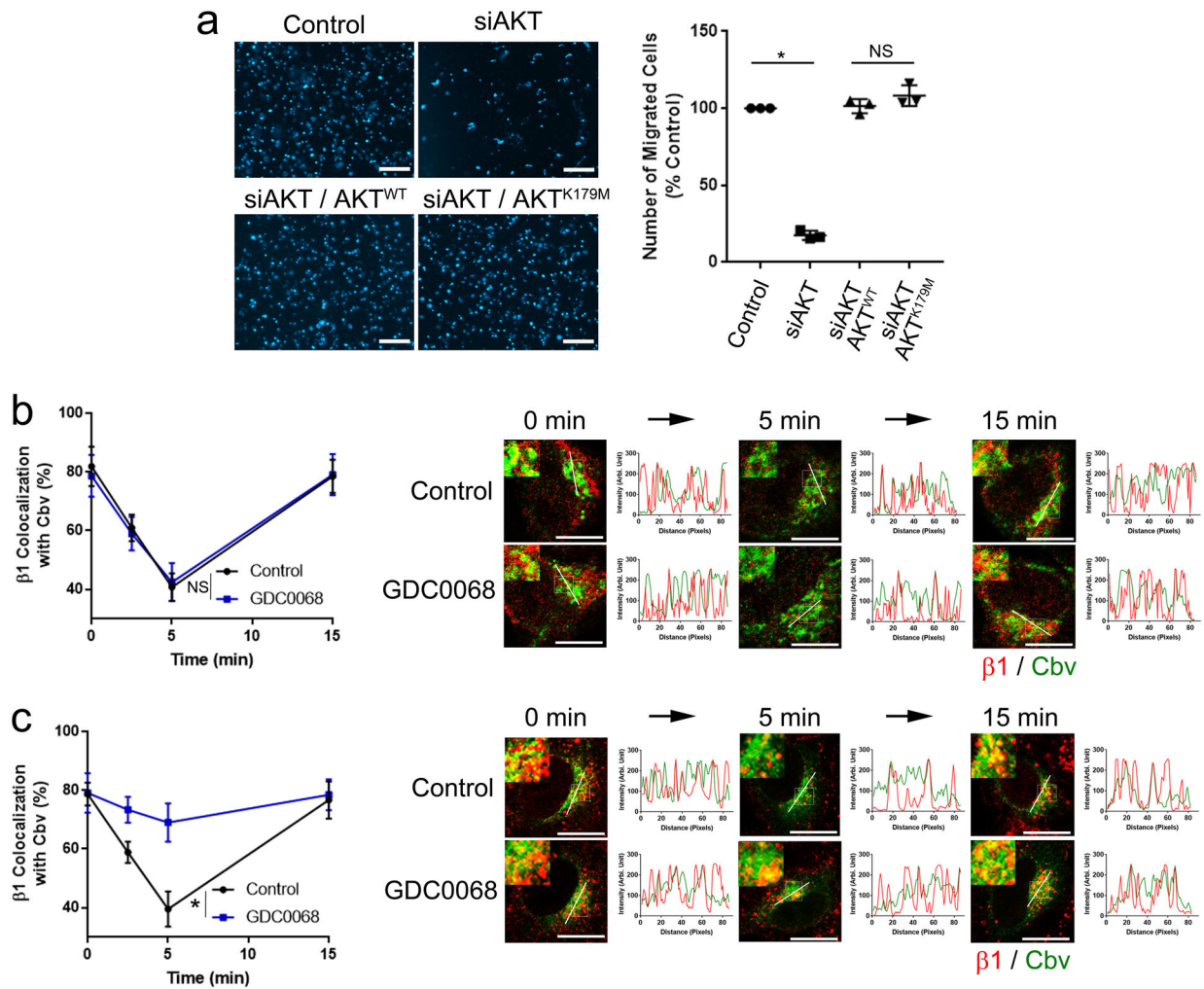
Extended Data Fig. 3. Further supporting a non-kinase role of Akt in integrin recycling.
a, Cell migration of the S554D-expressing HeLa cells as assessed through the transwell-based assay; n= 3 independent experiments, with each experiment examining three fields of transwell membranes. Primary images are shown on left, bar = 200 um. Quantitation is shown on right, mean +/− SD, *p=1.57×10^{-20}, NS p=0.125, paired two-tailed student's t-test. Data available in Source Data Extended Data Fig 3a. **b, c,** Integrin recycling assay assessing the effect of treating the S554D-expressing HeLa cells (**b**), or control HeLa cells (**c**), with the Akt kinase inhibitor GDC0068; n= 3 independent experiments. Quantitation is shown on left, mean +/− SD, with statistics performed for the 5-minute time point, NS p=0.248 (for analysis in **b**), *p=1.54×10^{-25} (for analysis in **c**), paired two-tailed student's t-test. Primary images, assessing the colocalization of endosomal β1 with cellubrevin (a marker of the recycling endosome), are shown on right, β1 (red), Cbv (green), bar = 10 um. Data available in Source Data Extended Data Fig 3b, 3c.
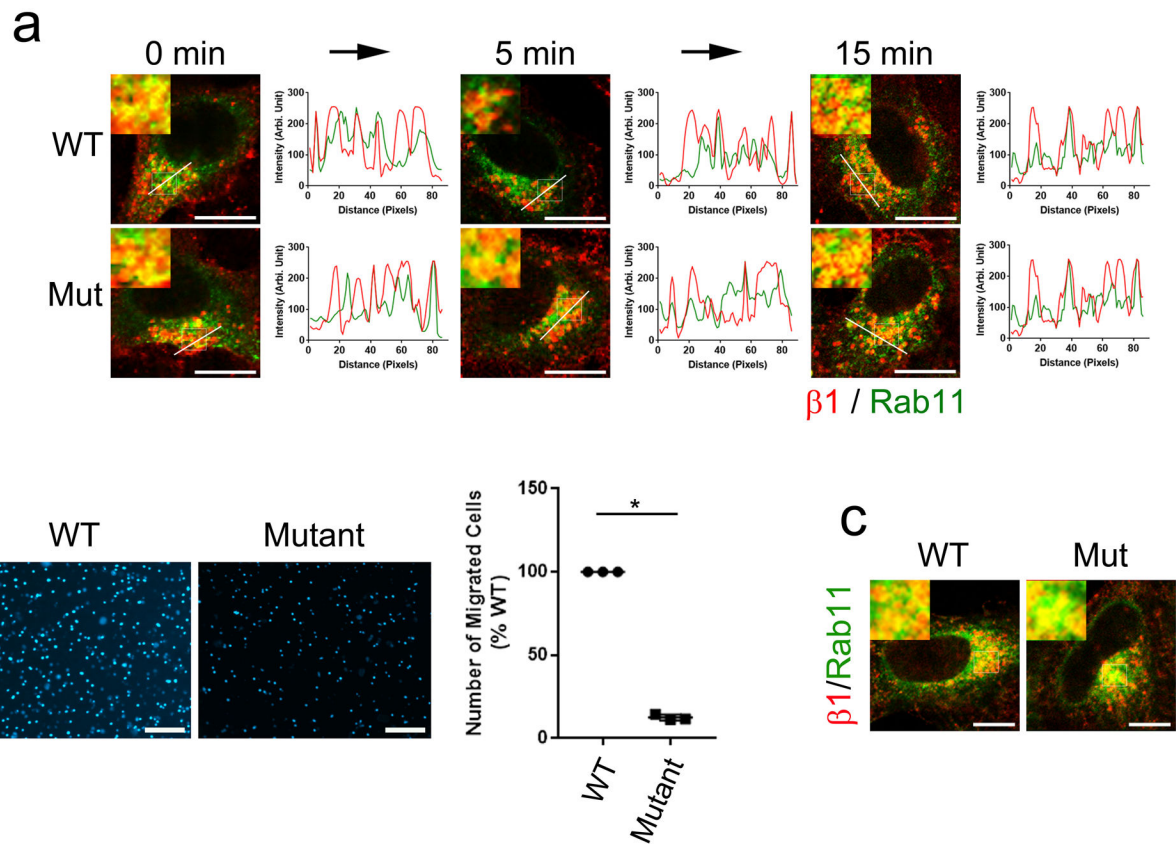
Extended Data Fig. 4. Further characterizing the effect of expressing a mutant α5 integrin.
a, Primary images from the integrin recycling assay shown in Figure 2d; n= 3 independent experiments. The colocalization of endosomal β1 with Rab11 is assessed; β1 (red), Rab11 (green), bar = 10 um. **b,** Cell migration of HeLa cells that express different α5 forms as assessed through the transwell-based assay; n= 3 independent experiments, with each experiment examining three fields of transwell membranes. Primary images are shown on left, bar = 200 um. Quantitation is shown on right, mean +/− SD, *p=2.08×10^{-24}, paired two-tailed student's t-test. Data available in Source Data Extended Data Fig 4b. **c,** Representative primary images for the colocalization study shown in Figure 2g; n= 3 independent experiments. The colocalization of endosomal β1 with Rab11 is assessed, β1 (red), Rab11 (green), bar = 10 um.
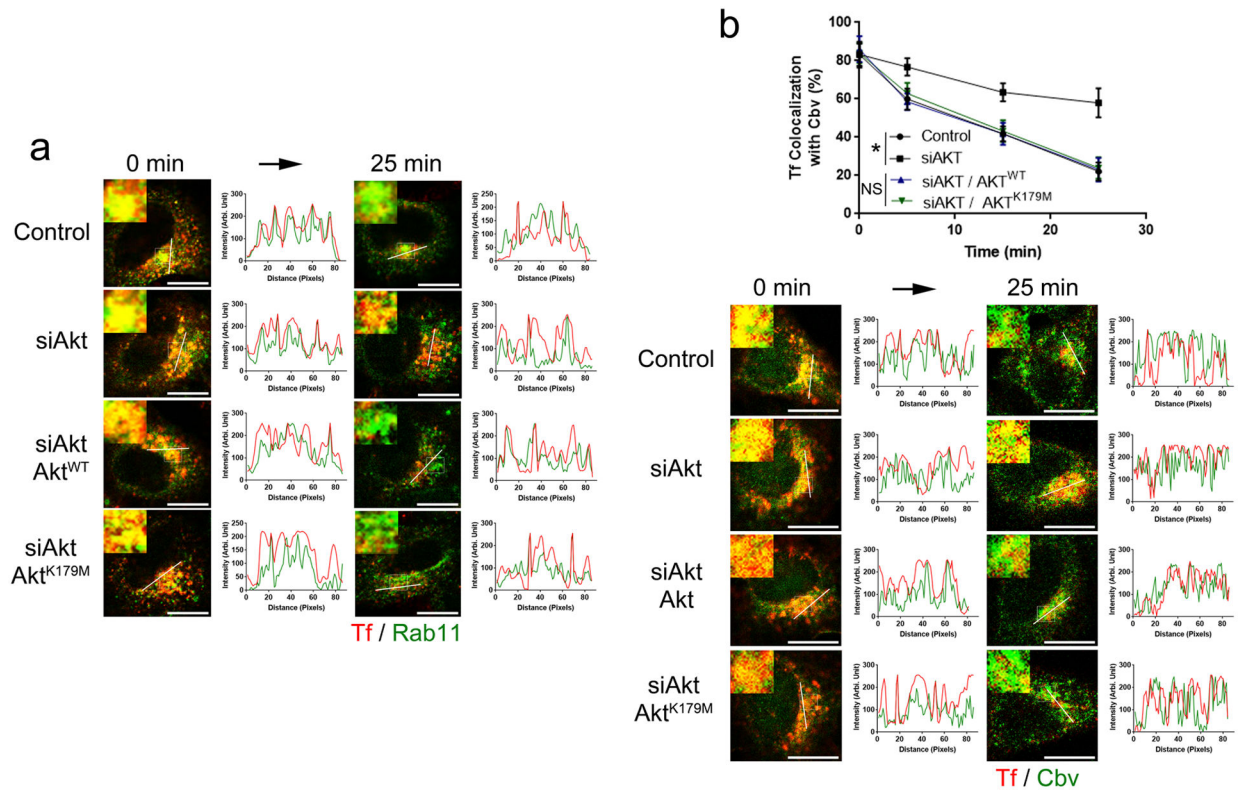
Extended Data Fig. 5. Further supporting a non-kinase role of Akt in TfR recycling.
a, Primary images from the TfR recycling assay shown in Figure 3a; n= 3 independent experiments. The colocalization of endosomal Tf with Rab11 is assessed; Tf (red), Rab11 (green), bar = 10 um. **b,** TfR recycling assay examining the effect of siRNA against Akt, and also rescue using wild-type (WT) or kinase-dead (K179M) Akt in HEK293 cells; n= 3 independent experiments, with each experiment examining 10 cells. Quantitation is shown above, mean +/− SD, with statistics performed on the 25-minute time point, *p=8.86×10^{-27}, NS p=0.557, paired two-tailed student's t-test. Primary images along with line scans are shown below, Tf (red), cellubrevin (green), bar = 10 um. Data available in Source Data Extended Data Fig 5b.
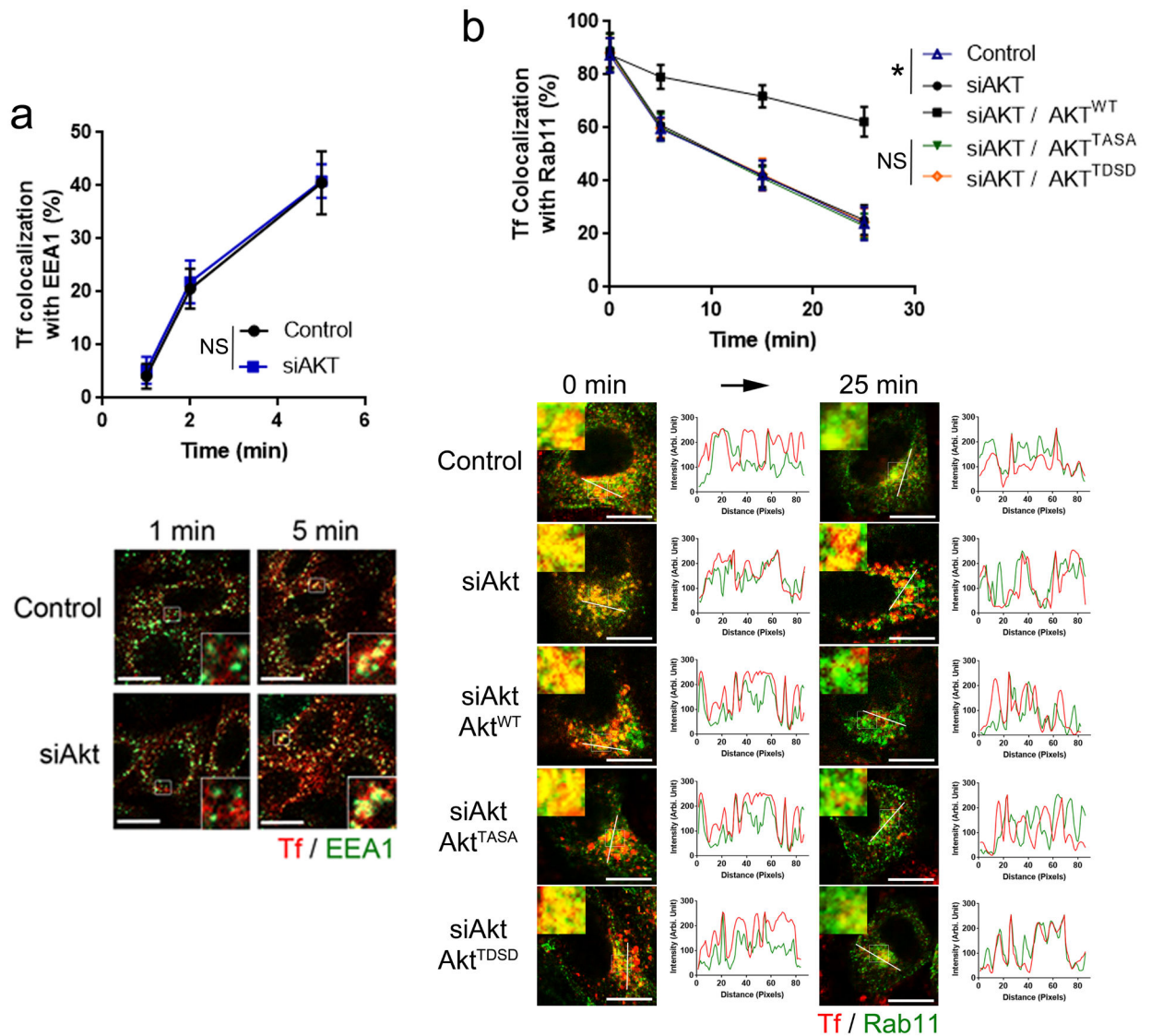
Extended Data Fig. 6. Further characterizing how Akt acts in the endocytic transport of TfR.
a, TfR internalization assay examining the effect of siRNA against Akt, n= 3 independent experiments, with each experiment examining 10 cells. Quantitation is shown above, mean +/− SD, with statistics performed for the 5-minute time point, NS p=0.538, paired two-tailed student's t-test. Primary images are shown below, Tf (red), EEA1 (a marker of the early endosome, green), bar = 10 um. Data available in Source Data Extended Data Fig 6a. **b,** TfR recycling assay examining the effect of siRNA against Akt, and also rescues using various forms of Akt in HeLa cells; n= 3 independent experiments, with each experiment examining 10 cells. Quantitation is shown above, mean +/− SD, with statistics performed on the 25-minute time point, *p=2.68×10^{-27}, NS p=0.303, paired two-tailed student's t-test. Primary images along with line scans are shown below, Tf (red), Rab11 (green), bar = 10 um. Data available in Source Data Extended Data Fig 6b.
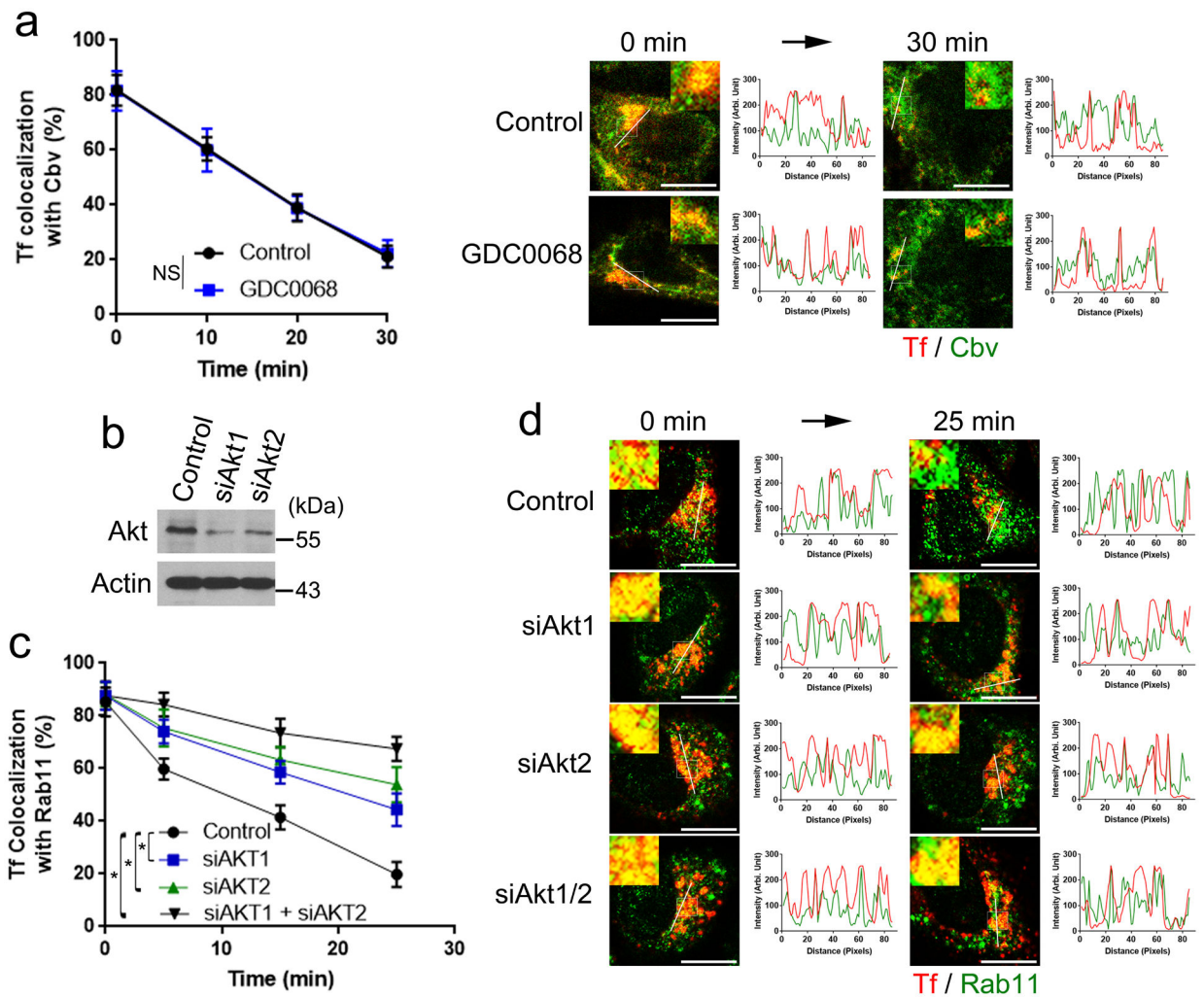
Extended Data Fig. 7. Further characterizing how Akt acts in TfR recycling.

a, TfR recycling assay examining the effect of treating HeLa cells with the Akt kinase inhibitor GDC0068; n= 3 independent experiments, with each experiment examining 10 cells. Quantitation is shown on left, mean +/− SD with statistics performed on the 30-minute time point, NS p=0.222, paired two-tailed student's t-test. Primary images along with line scans are shown on right; Tf (red), cellubrevin (green), bar = 10 um. Data available in Source Data Extended Data Fig 7a. **b,** Efficiency of siRNA against Akt1 and siRNA against Akt2 in HeLa cells, as assessed by immunoblotting of whole cell lysates; n= 2 independent experiments. Actin level confirms similar levels of cells examined. Data available in Unprocessed Blots Extended Data Fig 7b. **c, d,** TfR recycling assay examining the effect of siRNA against different isoforms of Akt in HeLa cells; n= 3 independent experiments, with each experiment examining 10 cells. Quantitation is shown in (**c**), mean +/− SD, with statistics performed on the 25-minute time point, *p=1.72×10^{-24} (control vs si-Akt1), *p=1.53×10^{-30} (control vs si-Akt2), *p=1.78×10^{-43} (control vs si-Akt1/si-Akt2), paired two-tailed student's t-test. Data available in Source Data Extended Data Fig 7c. Primary images along with line scans are shown in (**d**), Tf (red), Rab11 (green), bar = 10 um.

a

```
WT:  MMDQARSAFSNLFGGEPLSYTRFSLARQVDGDNSHVEMKLAVDEEENADNNTKANVTKPKR

N19: MMDQARSAFSNLFGGEPLS  YTRFSLARQVDGDNSHVEMKLAVDEEENADNNTKANVTKPKR  NΔ19
```

b

c

d
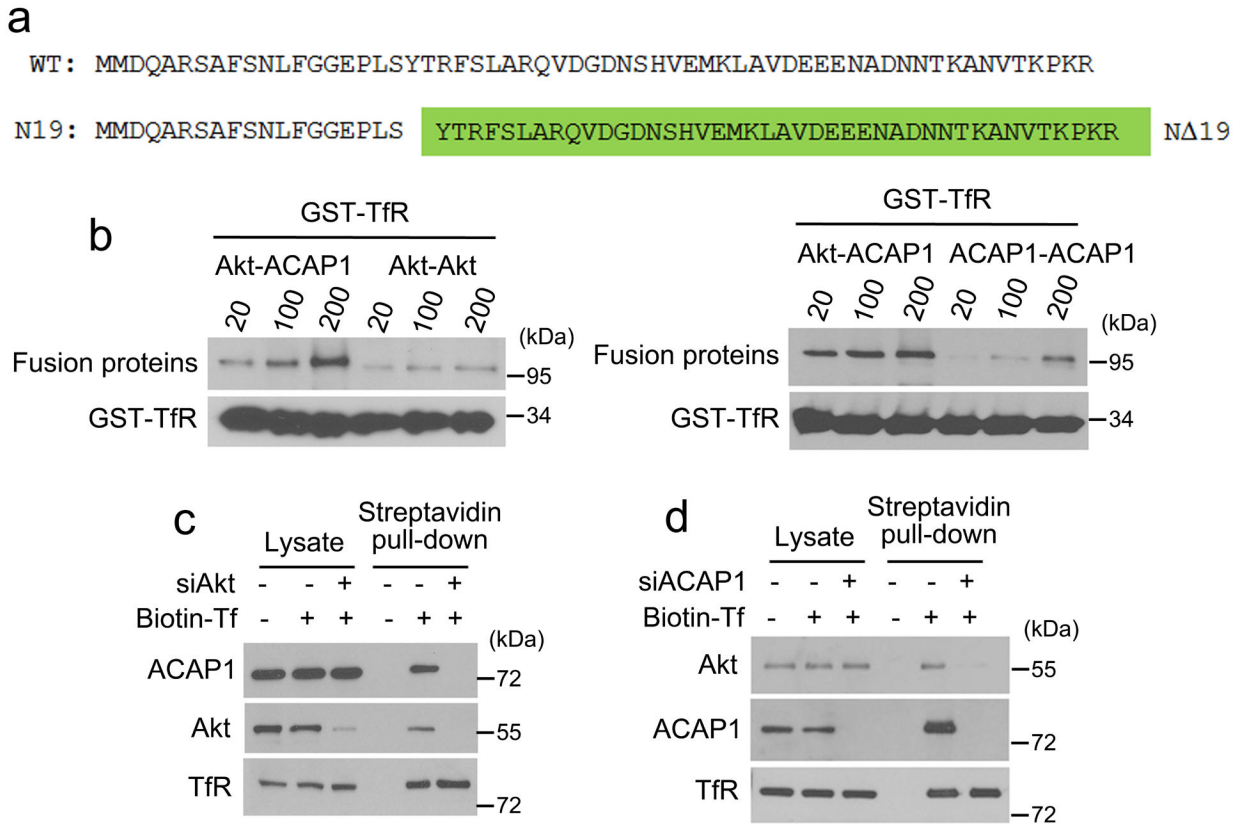
Extended Data Fig. 8. Further supporting Akt acts as a co-adaptor with ACAP1 in cargo binding.

a, Schematic showing the sequence of the TfR cytoplasmic domain, and the portions covered by the N19 and the N 19 constructs. **b,** Pulldown studies titrating increasing level of different fusion proteins of Akt and ACAP1 for their binding to the TfR cytoplasmic domain; n= 2 independent experiments. Left panel compares binding by Akt-ACAP1 heterodimer and Akt homodimer. Right panel compares binding by Akt-ACAP1 heterodimer and ACAP1 homodimer. Data available in Unprocessed Blots Extended Data Fig 8b. **c, d,** Co-precipitation studies examining the effect of siRNA against Akt on the association of endosomal TfR with ACAP1 and Akt in HeLa cells (**c**), and siRNA against ACAP1 on the association of endosomal TfR with Akt and ACAP1 in HeLa cells (**d**); n= 2 independent experiments. Biotin-labeled Tf was internalized for 2 hours to label the endosomal pool of TfR. Immunoblotting of whole cell lysates confirms the efficiency of siRNA treatment. Data available in Unprocessed Blots Extended Data Fig 8c, 8d.
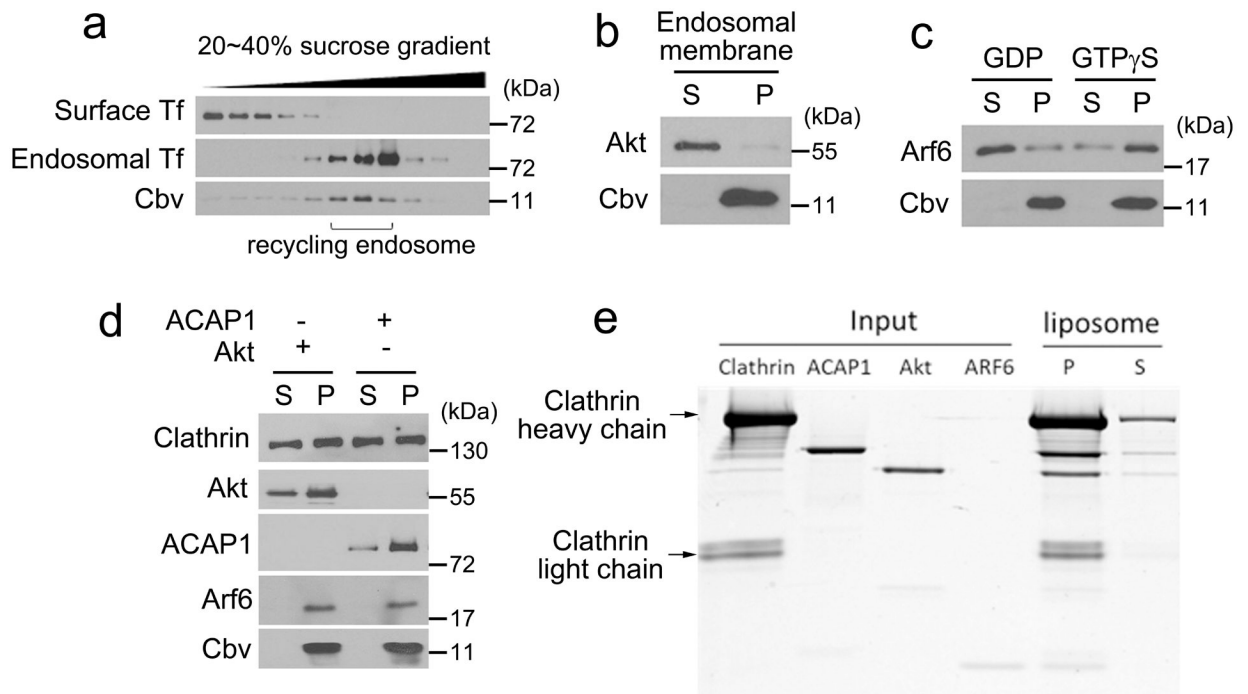
Extended Data Fig. 9. Further characterizing membrane recruitment of Akt.
a, Isolating a membrane fraction from HeLa cells enriched for the recycling endosome using a sucrose gradient established through equilibrium centrifugation; n= 2 independent experiments. Fractions enriched for the recycling endosome were identified by tracking cellubrevin and internalized Tf (which bound to endosomal TfR), and not surface Tf (which bound to surface TfR). Data available in Unprocessed Blots Extended Data Fig 9a. **b, c, d,** Recruitment studies showing that Akt alone cannot be recruited to endosomal membrane (**b**), while ARF6 alone in its activate form can be recruited to endosomal membrane (**c**), and clathrin recruitment to endosomal membrane requires ARF6 with either Akt or ACAP1 (**d**); n= 2 independent experiments. Cellubrevin tracks endosomal membrane. Data available in Unprocessed Blots Extended Data Fig 9b, 9c, 9d. **e,** Recruitment study examining the relative levels of ARF6, Akt, ACAP1, and clathrin recruited to liposomes; n= 2 independent experiments. Input shows the total amount of each component added for the incubation. Data available in Unprocessed Blots Extended Data Fig 9e.
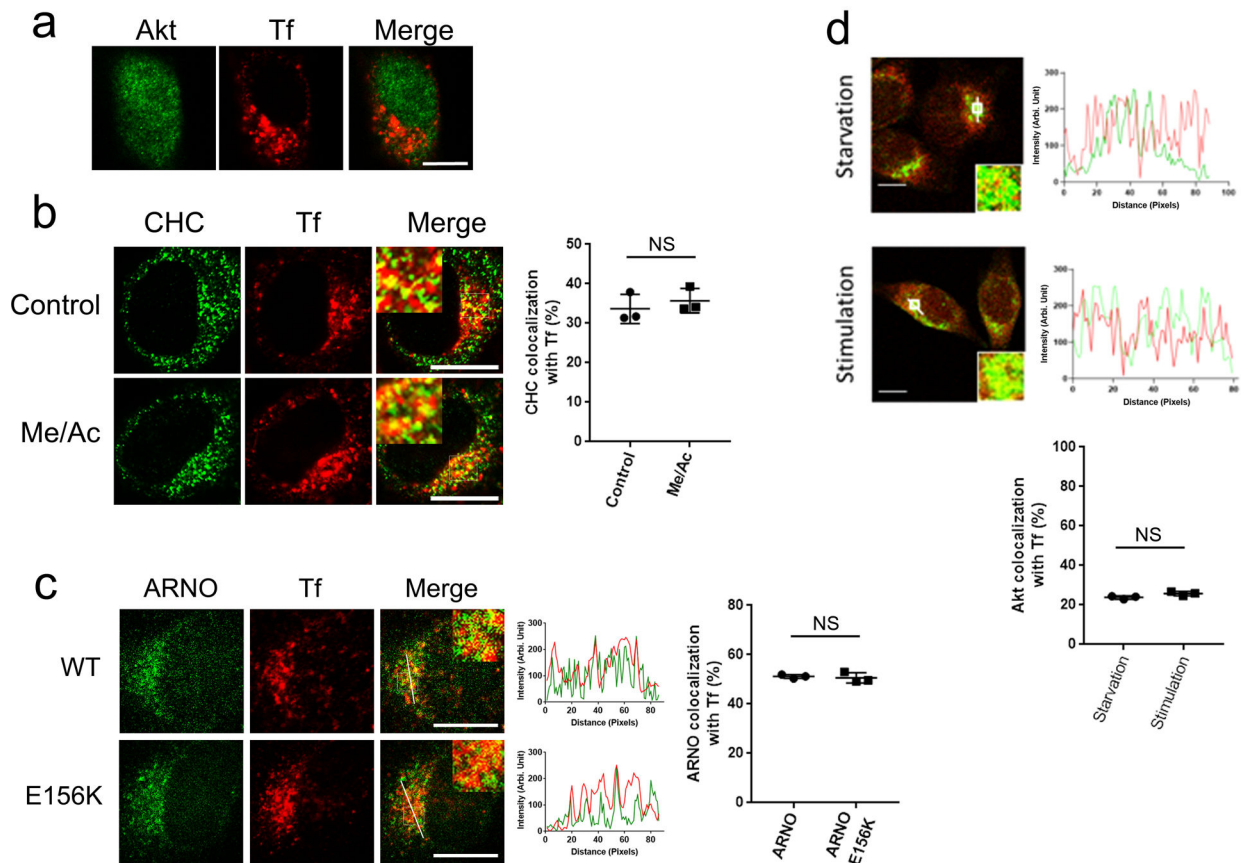
Extended Data Fig. 10. Further characterizing endogenous Akt at the recycling endosome.
a, Confocal microscopy examining the colocalization of endogenous Akt with endosomal Tf in HeLa cells; n= 3 independent experiments, with each experiment examining 10 cells. Primary images are shown, Akt (green), Tf (red), bar = 10 um. **b,** Confocal microscopy examining the effect of a more denaturing fixative (containing methanol and acetone) on the ability to detect endogenous clathrin at the recycling endosome in HeLa cells; n= 3 independent experiments, with each experiment examining 10 cells. Primary images along with line scan are shown on left for the colocalization of clathrin with endosomal Tf, clathrin (green), Tf (red), bar = 10 um. Quantitation is shown on right, mean +/− SD, NS p=0.106, paired two-tailed student's t-test. Data available in Source Data Extended Data Fig 10b. **c,** Confocal microscopy examining the colocalization of different forms of ARNO with endosomal Tf in HeLa cells; n= 3 independent experiments, with each experiment examining 10 cells. Primary images along with line scan are shown on left for the colocalization of endogenous Akt with endosomal Tf, ARNO (green), Tf (red), bar = 10 um. Quantitation is shown on right, mean +/− SD, NS p=0.686, paired two-tailed student's t-test. Data available in Source Data Extended Data Fig 10c. **d,** Confocal microscopy examining the effect of serum stimulation on Akt localization at the recycling endosome in HeLa cells; n= 3 independent experiments, with each experiment examining 10 cells. Primary images along with line scan are shown above for the colocalization of endogenous Akt with endosomal Tf, Akt (red), Tf (green), bar = 10 um. Quantitation is shown below, mean +/−

SD, NS p=0.325, paired two-tailed student's t-test. Data available in Source Data Extended Data Fig 10d.

Acknowledgements

References

1. Robinson MS Adaptable adaptors for coated vesicles. Trends Cell Biol 14, 167–174 (2004). [PubMed: 15066634]

2. Traub LM Tickets to ride: selecting cargo for clathrin-regulated internalization. Nat Rev Mol Cell Biol 10, 583–596 (2009). [PubMed: 19696796]

3. Miller EA & Barlowe C Regulation of coat assembly--sorting things out at the ER. Curr Opin Cell Biol 22, 447–453 (2010). [PubMed: 20439155]

4. Dai J et al. ACAP1 Promotes Endocytic Recycling by Recognizing Recycling Sorting Signals. Dev Cell 7, 771–776 (2004). [PubMed: 15525538]

5. Li J et al. Phosphorylation of ACAP1 by Akt regulates the stimulation-dependent recycling of integrin beta1 to control cell migration. Dev Cell 9, 663–673 (2005). [PubMed: 16256741]

6. Li J et al. An ACAP1-containing clathrin coat complex for endocytic recycling. J Cell Biol 178, 453–464 (2007). [PubMed: 17664335]

7. Caswell P & Norman J Endocytic transport of integrins during cell migration and invasion. Trends Cell Biol 18, 257–263 (2008). [PubMed: 18456497]

8. Grant BD & Donaldson JG Pathways and mechanisms of endocytic recycling. Nat Rev Mol Cell Biol 10, 597–608 (2009). [PubMed: 19696797]

9. Hsu VW, Bai M & Li J Getting active: protein sorting in endocytic recycling. Nat Rev Mol Cell Biol 13, 323–328 (2012). [PubMed: 22498832]

10. Irannejad R & von Zastrow M GPCR signaling along the endocytic pathway. Curr Opin Cell Biol 27, 109–116 (2014). [PubMed: 24680436]

11. Rodriguez-Boulan E & Macara IG Organization and execution of the epithelial polarity programme. Nat Rev Mol Cell Biol 15, 225–242 (2014). [PubMed: 24651541]

12. Cullen PJ & Steinberg F To degrade or not to degrade: mechanisms and significance of endocytic recycling. Nat Rev Mol Cell Biol 19, 679–696 (2018). [PubMed: 30194414]

13. Bai M et al. Mechanistic Insights into Regulated Cargo Binding by ACAP1 Protein. J Biol Chem 287, 28675–28685 (2012). [PubMed: 22645133]

14. Bonifacino JS & Traub LM Signals for sorting of transmembrane proteins to endosomes and lysosomes. Annu Rev Biochem 72, 395–447 (2003). [PubMed: 12651740]

15. Manning BD & Toker A AKT/PKB Signaling: Navigating the Network. Cell 169, 381–405 (2017). [PubMed: 28431241]

16. Alessi DR et al. Mechanism of activation of protein kinase B by insulin and IGF-1. Embo J 15, 6541–6551 (1996). [PubMed: 8978681]

17. Oh SJ & Santy LC Differential effects of cytohesins 2 and 3 on beta1 integrin recycling. J Biol Chem 285, 14610–14616 (2010). [PubMed: 20223830]

18. Rosselli-Murai LK et al. Loss of PTEN promotes formation of signaling-capable clathrin-coated pits. J Cell Sci 131 (2018).

19. Cao TT, Deacon HW, Reczek D, Bretscher A & von Zastrow M A kinase-regulated PDZ-domain interaction controls endocytic sorting of the beta2-adrenergic receptor. Nature 401, 286–290 (1999). [PubMed: 10499588]

20. Conner SD & Schmid SL Identification of an adaptor-associated kinase, AAK1, as a regulator of clathrin-mediated endocytosis. J Cell Biol 156, 921–929 (2002). [PubMed: 11877461]

21. Kuroda F, Moss J & Vaughan M Regulation of brefeldin A-inhibited guanine nucleotide-exchange protein 1 (BIG1) and BIG2 activity via PKA and protein phosphatase 1gamma. Proc Natl Acad Sci U S A 104, 3201–3206 (2007). [PubMed: 17360629]

22. Liberali P et al. The closure of Pak1-dependent macropinosomes requires the phosphorylation of CtBP1/BARS. Embo J 27, 970–981 (2008). [PubMed: 18354494]

23. Weller SG et al. Src kinase regulates the integrity and function of the Golgi apparatus via activation of dynamin 2. Proc Natl Acad Sci U S A 107, 5863–5868 (2010). [PubMed: 20231454]

24. Ren J & Guo W ERK1/2 regulate exocytosis through direct phosphorylation of the exocyst component Exo70. Dev Cell 22, 967–978 (2012). [PubMed: 22595671]

25. Luo G, Zhang J, Luca FC & Guo W Mitotic phosphorylation of Exo84 disrupts exocyst assembly and arrests cell growth. J Cell Biol 202, 97–111 (2013). [PubMed: 23836930]

26. Xiao GY, Mohanakrishnan A & Schmid SL Role for ERK1/2-dependent activation of FCHSD2 in cancer cell-selective regulation of clathrin-mediated endocytosis. Proc Natl Acad Sci U S A 115, E9570–E9579 (2018). [PubMed: 30249660]

27. Yang JS et al. GAPDH inhibits intracellular pathways during starvation for cellular energy homeostasis. Nature 561, 263–267 (2018). [PubMed: 30209366]

28. Powelka AM et al. Stimulation-Dependent Recycling of Integrin beta1 Regulated by ARF6 and Rab11. Traffic 5, 20–36 (2004). [PubMed: 14675422]
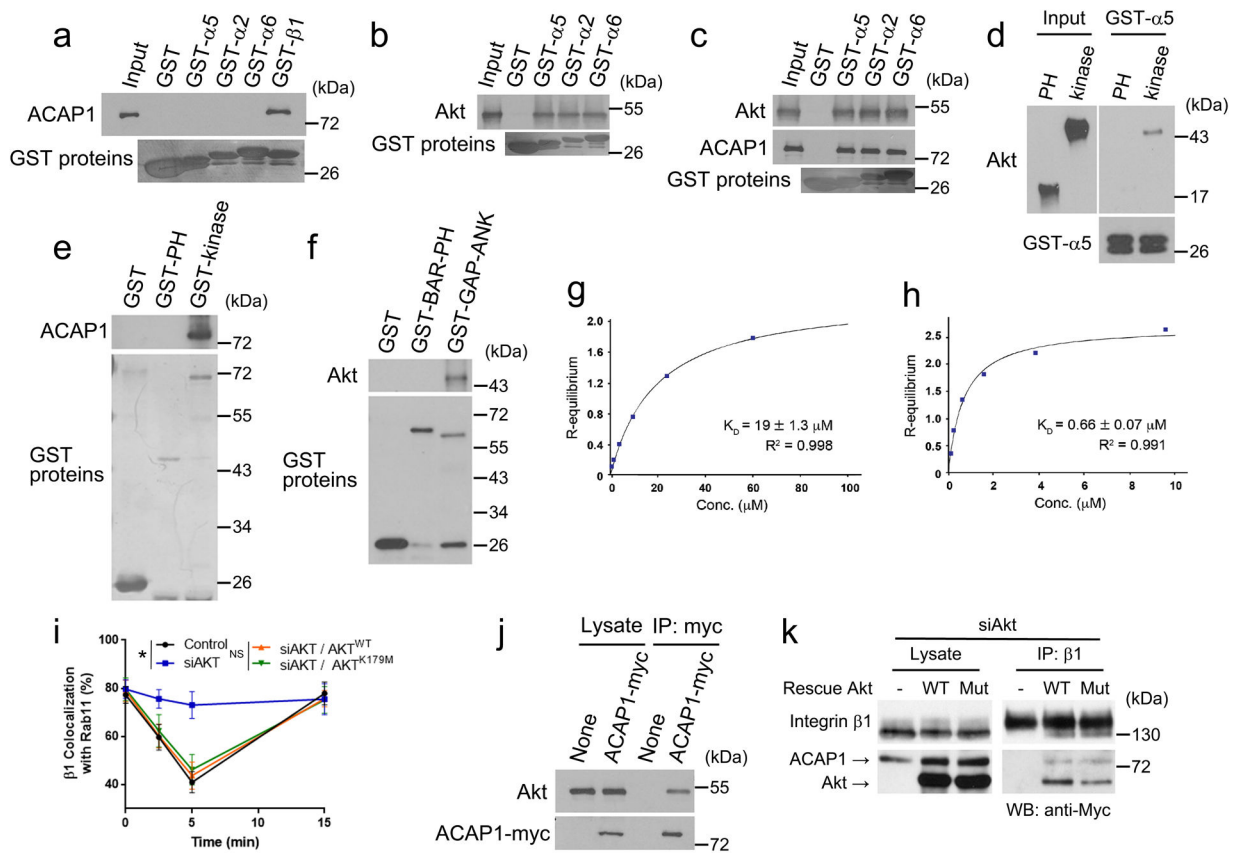
Figure 1. Akt binds to integrin and ACAP1.
a, b, c, Pulldown studies examining Akt and/or ACAP1 binding to integrin tails, as assessed by immunoblotting; n= 2 independent experiments. Input shows 15% of soluble components used in the incubation. Data available in Unprocessed Blots Fig 1a, 1b, 1c. **d, e, f,** Pulldown studies examining interactions through immunoblotting: Akt binding to GST-α5 (**d**), soluble ACAP1 binding to Akt forms as GST fusions (**e**), or Akt binding to ACAP1 forms as GST fusions (**f**); n= 2 independent experiments. In (**d**), input shows 50% of soluble components used in the incubation. Data available in Unprocessed Blots Fig 1d, 1e, 1f. **g, h,** Biolayer interferometry quantifying the interaction between GST-α5 and the Akt kinase domain (**g**), or between the Akt kinase domain and the carboxyl portion of ACAP1 (**h**); n= 2 independent experiments. Double reference subtracted binding curves generated from 6 data points were analyzed to obtain binding constant (K_D) values using globally fit 1:1 Langmuir binding model, which are expressed as mean +/− standard error (SEM). Data available in Source Data Fig 1g, 1h. **i,** Integrin recycling assay performed on HeLa cells that express the S554D mutant of ACAP1, examining the effect of siRNA against Akt, and rescue using wild-type (WT) or kinase-dead (K179M) form of Akt; n= 3 independent experiments, with each experiment examining 10 cells. Mean +/− standard deviation (SD), with statistics performed for the 5-minute time point, *p=1.87×10^{-31}, NS (non-significant) p=0.112, paired two-tailed student's t-test. Data available in Source Data Fig 1i. **j,** Co-precipitation study examining the interaction of transfected myc-tagged ACAP1 with endogenous Akt in HeLa cells; n= 2 independent experiments. Data available in Unprocessed Blots Fig 1j. **k,** Co-precipitation

study examining the effect of siRNA against Akt on the formation of a complex that contains endosomal β1, ACAP1, and Akt in the S554D-expressing HeLa cells; n= 2 independent experiments. The mutant ACAP1 is myc-tagged and rescues are done using myc-tagged forms of Akt. Thus, immunoblotting using an anti-myc antibody detects both ACAP1 and Akt. Data available in Unprocessed Blots Fig 1k.
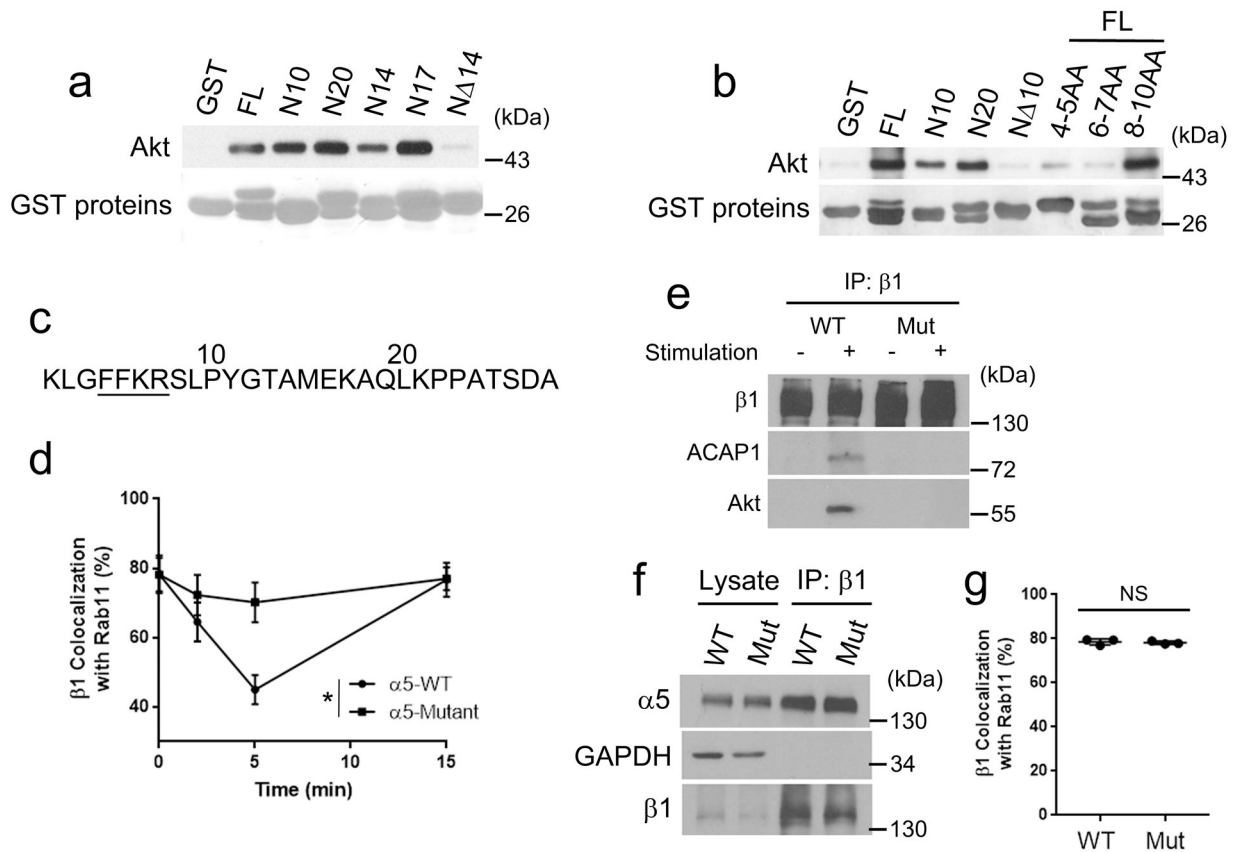
Figure 2. Akt recognizes a recycling sorting signal in the α5 tail.
a,b, Pulldown studies examining Akt binding to truncation or point mutants of the α5 tail as GST fusions; n= 2 independent experiments. Truncation forms are defined with respect to the sequence shown in Figure 2c; FL (full-length), N10 (first 10 aa), N20 (first 20 aa), N14 (first 14 aa), N17 (first 17 aa), NΔ14 (lacking the first 14 aa), NΔ10 (lacking the first 10 aa), FL/4–5AA (full-length with residues 4 and 5 replaced by alanines), FL/6–7AA (full-length with residues 6 and 7 replaced by alanines), FL/8–10AA (full-length with residues 8, 9, 10 replaced by alanines). Data available in Unprocessed Blots Fig 2a, 2b. **c,** A schematic showing residues of the α5 tail, with numbering starting with the most membrane proximal residue. Residues underlined are required for Akt binding. **d,** Integrin recycling assay performed on HeLa cells that express different α5 forms; n= 3 independent experiments, with each experiment examining 10 cells. Mean +/− SD, with statistics performed for the 5-minute time point, *p=7.8×10^{-26}, paired two-tailed student's t-test. Data available in Source Data Fig 2d. **e,** Co-precipitation studies examining the effect of expressing the mutant α5 on the formation of a complex containing endosomal β1, ACAP1 and Akt in HeLa cells; n= 2 independent experiments. Data available in Unprocessed Blots Fig 2e. **f,** Co-precipitation studies examining α5β1 heterodimerization in HeLa cells that express either wild-type or mutant α5; n= 2 independent experiments. Data available in Unprocessed Blots Fig 2f. **g,** Confocal microscopy examining the colocalization of the α5β1 integrin (as tracked through β1) and Rab11 (a marker of the recycling endosome) in HeLa cells that express either wild-type or mutant α5; n= 3 independent experiments, with each experiment examining 10 cells.

Mean +/− SD, NS p=0.402, paired two-tailed student's t-test. Data available in Source Data Fig 2g.
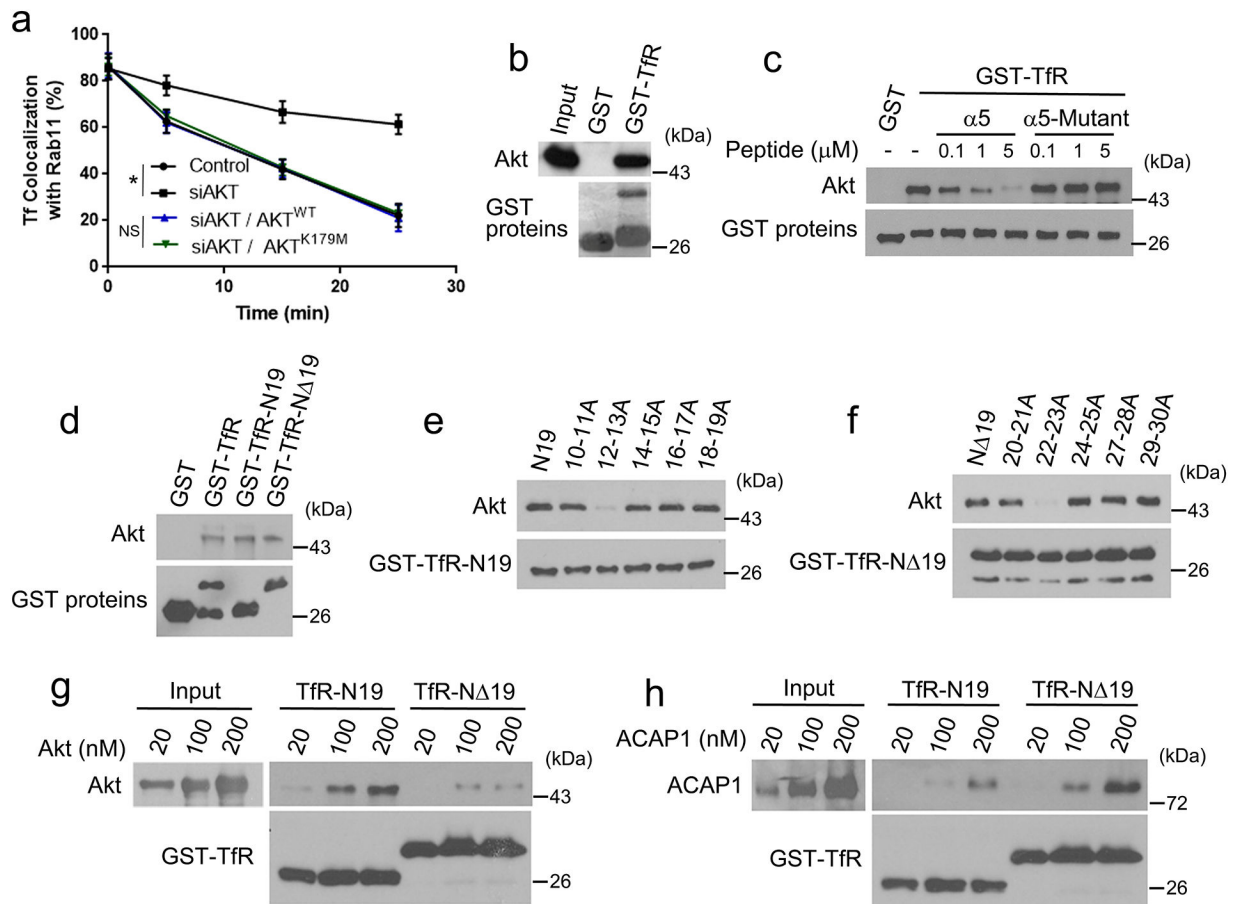
Figure 3. Akt acts in the cargo sorting of TfR to promote its recycling.
a, TfR recycling assay examining the effect of siRNA against Akt, and rescue using wild-type (WT) or kinase-dead (K179M) Akt in HeLa cells; n= 3 independent experiments, with each experiment examining 10 cells. Mean +/− SD, with statistics performed on the 25-minute time point, $*p=1.69\times10^{-38}$, NS p=0.161, paired two-tailed student's t-test. Data available in Source Data Fig 3a. **b,** Pulldown study examining Akt binding to the TfR cytoplasmic domain; n= 2 independent experiments. Input shows 10% of the soluble amount used in the incubation. Data available in Unprocessed Blots Fig 3b. **c,** Pulldown study examining the effect of titrating increasing level of a α5 cargo peptide (wild-type or mutant that cannot bind Akt), on Akt binding to the TfR cytoplasmic domain on beads; n= 2 independent experiments. Data available in Unprocessed Blots Fig 3c. **d, e, f,** Pulldown studies examining Akt binding to truncation form of the TfR cytoplasmic domain (**d**), to point mutants of the TfR-N19 construct (**e**), or to the point mutants of the TfR-N 19 construct (**f**); n= 2 independent experiments. Data available in Unprocessed Blots Fig 3d, 3e, 3f. **g, h,** Pulldown studies titrating increasing level of Akt for binding to TfR-N19 or TfR-N 19 (**g**), or increasing level of ACAP1 for binding to these two TfR constructs (**h**); n= 2 independent experiments. Data available in Unprocessed Blots Fig 3g, 3h.
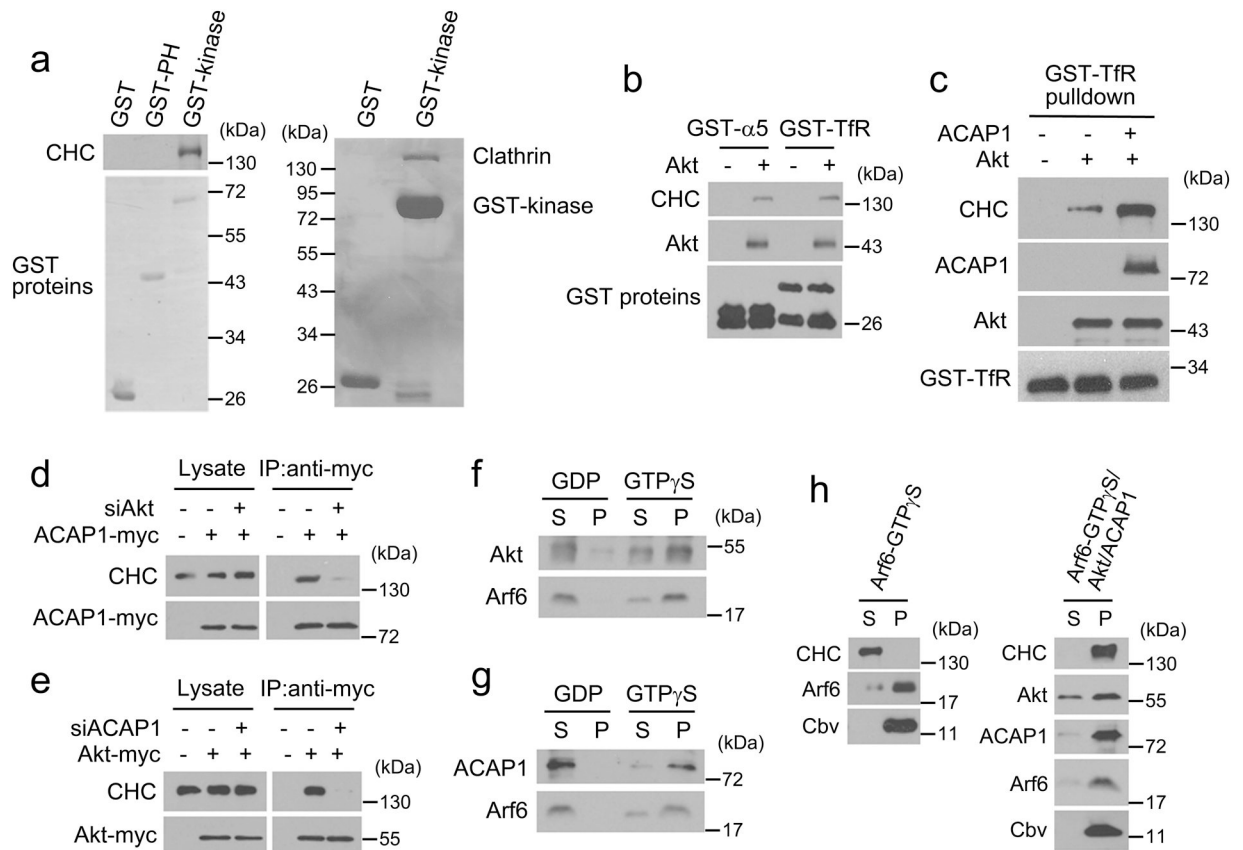
Figure 4. Akt links clathrin to cargoes and mediates clathrin recruitment to endosomal membrane.

a, Pulldown studies examining clathrin binding to domains of Akt; n= 2 independent experiments. Binding was assessed by either immunoblotting (left panel) or Coomassie staining (right panel). Data available in Unprocessed Blots Fig 4a, 4b. **b, c,** Pulldown studies examining the effect of having Akt (**b**) or Akt and ACAP1 (**c**) being present on clathrin binding to cargoes; n= 2 independent experiments. Data available in Unprocessed Blots Fig 4b, 4c. **d, e,** Co-precipitation studies examining the effect of siRNA against Akt on the association of clathrin with ACAP1 in HeLa cells (**d**) or siRNA against ACAP1 on the association of clathrin with Akt in HeLa cells (**e**); n= 2 independent experiments. Data available in Unprocessed Blots Fig 4d, 4e. **f, g,** Recruitment studies showing Akt recruitment to endosomal membrane requiring activated ARF6 (**f**), or ACAP1 recruitment to endosomal membrane requiring activated ARF6 (**g**); n= 2 independent experiments. Membrane fraction is tracked by the presence of cellubrevin. Data available in Unprocessed Blots Fig 4f, 4g. **h,** Recruitment studies examining clathrin recruitment to endosomal membrane with respect to the presence of ARF6 (left panel), or the additional presence of Akt and ACAP1 (right panel); n= 2 independent experiments. Membrane fraction is tracked by the presence of cellubrevin. Data available in Unprocessed Blots Fig 4h.
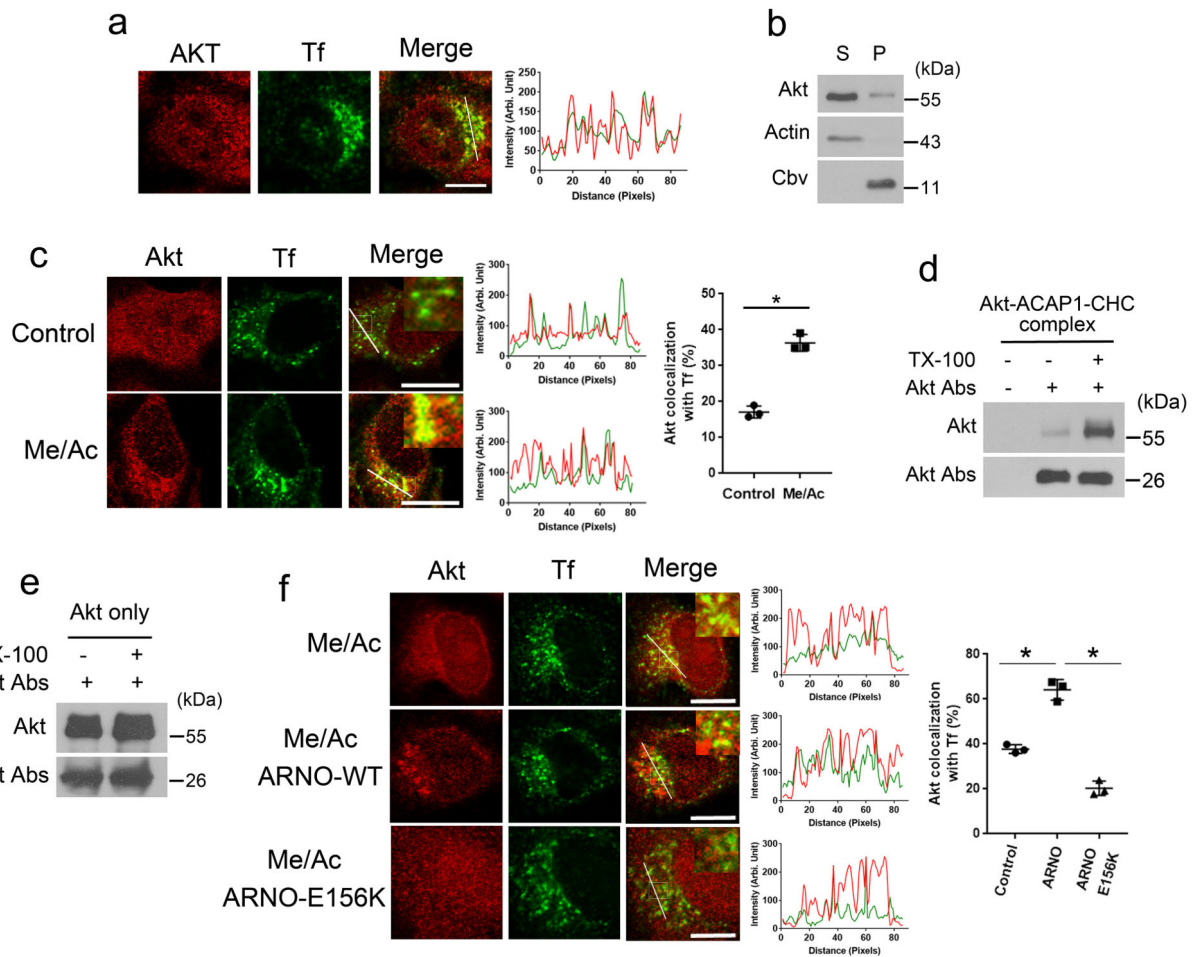
Figure 5. Akt at the recycling endosome exists mostly within assembled complexes.
a, Confocal microscopy examining the colocalization of endogenous Akt with the endosomal pool of transferrin (Tf) in HeLa cells; n= 3 independent experiments, with each experiment examining 10 cells. Primary images along with line scan are shown, Akt (red), Tf (green), bar = 10 um. **b,** Subcellular fractionation of HeLa cells assessing the relative distribution of endogenous Akt in the total membrane versus the cytosol fraction; n= 2 independent experiments. Actin tracks cytosol, while cellubrevin tracks endosomal membrane. Data available in Unprocessed Blots Fig 5b. **c,** Confocal microscopy examining the effect of a more denaturing fixative (containing methanol and acetone) in detecting endogenous Akt at the recycling endosome in HeLa cells; n= 3 independent experiments, with each experiment examining 10 cells. Primary images along with line scan are shown on left for the colocalization of Akt with endosomal Tf, Akt (red), Tf (green), bar = 10 um. Quantitation is shown on right, mean +/− SD, *p=1.18×10^{-22}, paired two-tailed student's t-test. Data available in Source Data Fig 5c. **d, e,** An antibody-based assay to detect Akt assembled on endosomal membrane; n= 2 independent experiments. Akt along with ACAP1, and clathrin (**d**), or Akt alone (**e**) is recruited to endosomal membrane in an ARF6-dependent fashion. An Akt antibody is then incubated with the membrane, either before or after membrane solubilization with detergent, followed by isolation of the antibody to detect

associated Akt. Data available in Unprocessed Blots Fig 5d, 5e. **f,** Confocal microscopy examining the effect of overexpressing either wild-type (WT) or catalytic-dead (E156K) ARNO on the ability to detect endogenous Akt at the recycling endosome in HeLa cells; n= 3 independent experiments, with each experiment examining 10 cells. Primary images along with line scan are shown on left for the colocalization of Akt with endosomal Tf, Akt (red), Tf (green), bar = 10 um. Quantitation is shown on right, mean +/− SD, *p=1.57×10^{-24} (no ARNO vs ARNO), *p=1.56×10^{-37} (ARNO WT vs ARNO E156K), paired two-tailed student's t-test. Data available in Source Data Fig 5f.